

Sensorless from standstill with high torque for synchronous motors exhibiting saliency

B.M. Putter

bmp72@hotmail.com

This slide set discusses a method for sensorless motor control, from standstill and after a cold start / reset. The method can be inaudible and provides unquantized phase information to a FOC motor control block. The motor can be driven uninterruptedly with full torque, while the algorithm runs in the background.

Apart from the illustration on slide 5 (which I once encountered in a google image search) all work was performed independently and unhindered by knowledge of motor control literature. I do not work in the field of motor control professionally and am not familiar with the state of the art. Motor control literature was not consulted, therefore there are no references.

Apart from things already claimed and/or patented by other parties unknown to me, the work presented here is placed in the public domain. I do not claim ownership of the discussed algorithms and methods. No liability is accepted, use at your own risk !

If you like this slide set and find the information it contains useful, please make a Paypal donation to bmp72@hotmail.com

Bas Putter,
Adliswil, Switzerland

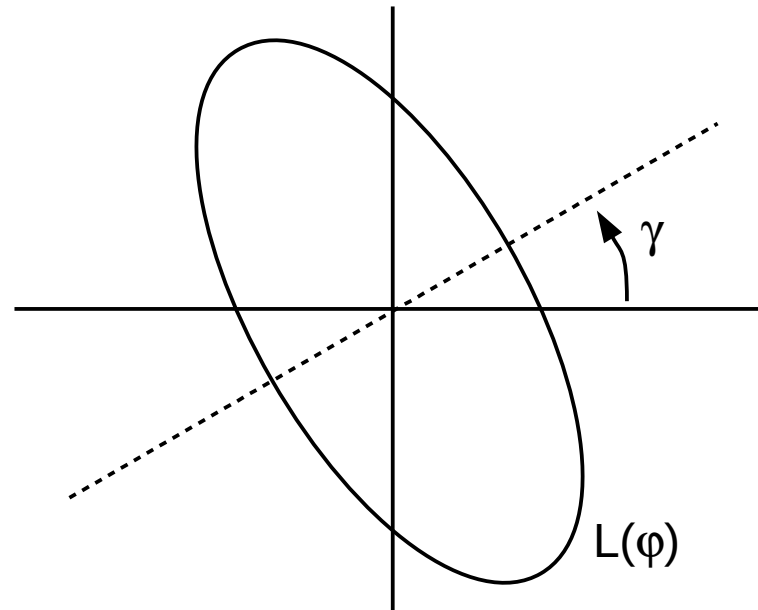
Overview

- Basic principle
- Using the PWM frequency
- The Magnetic Circle Vector
- Determining the MSB
- Sector switching
- Use with FOC
- Verifying Saliency angle with Back EMF

Overview

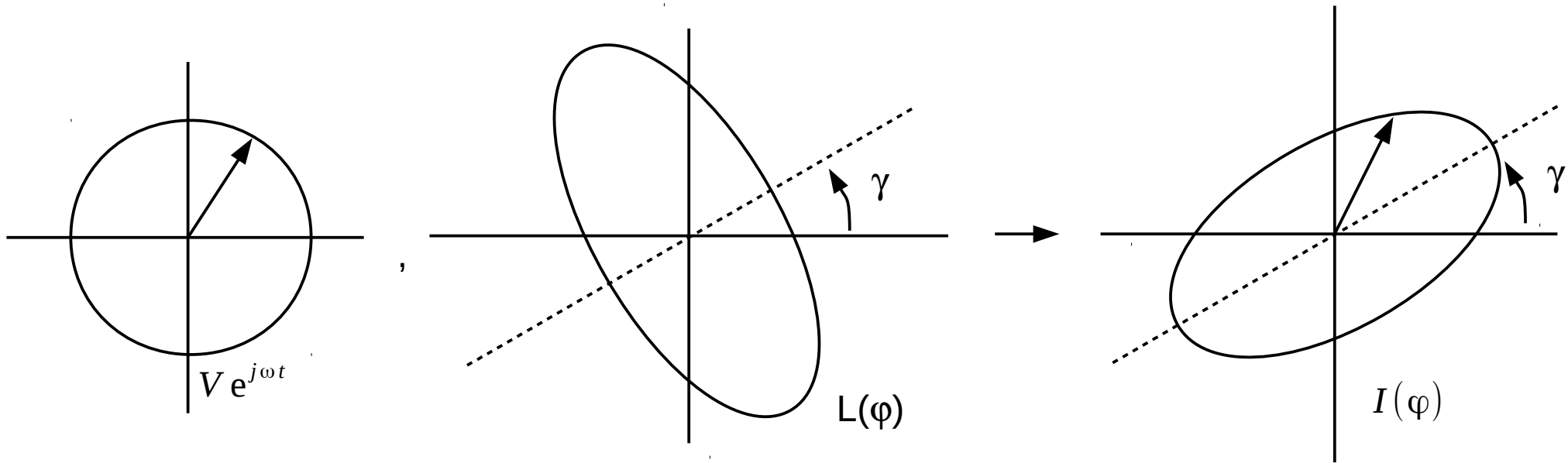
- Appendices
 - A: Clarke Transform
 - B: Receiver structure
 - C: Making TX signals real
 - D: Low side current sensing
 - E: Frequency selection
 - F: Hardware used and demo videos

Basic principle



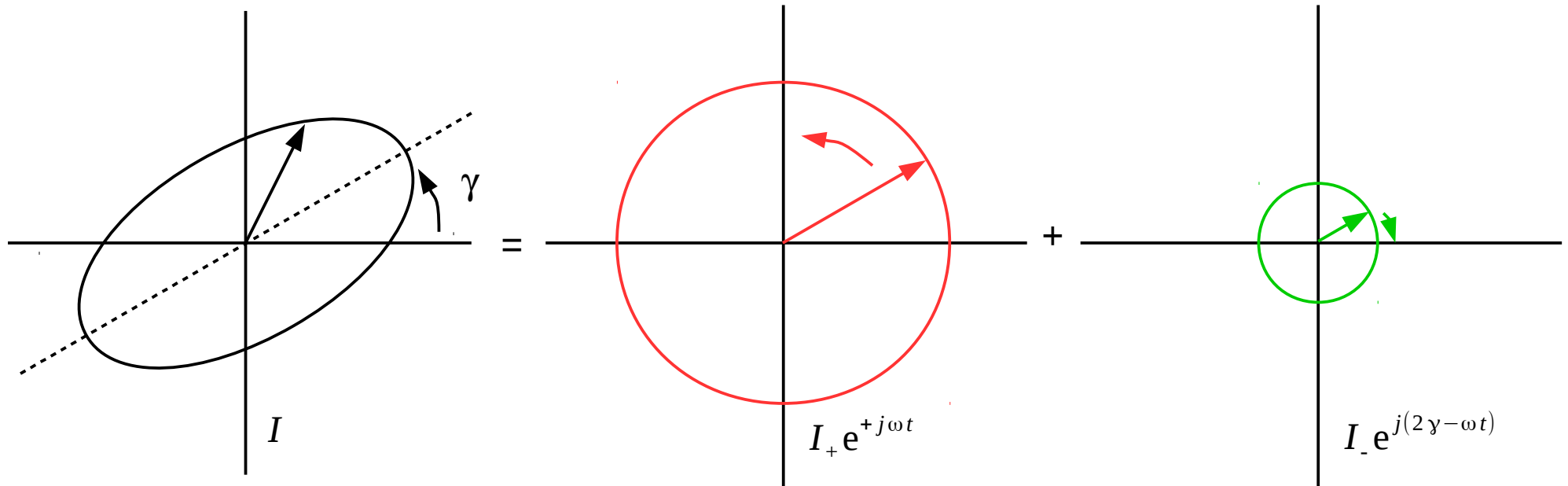
- Instead of observing three different inductors, the motor inductance L can be treated as a single electrical angle (φ) dependent inductance.
- This will be an elliptic shape tilted at angle γ , with γ the angle of the rotor magnets. The rotor magnets partly saturate the stator iron, reducing the motor inductance at angle γ and causing the elliptic shape.
- In the following slides it is assumed the motor inductance is the only cause of voltage to current transfer differences between the 3 motor channels.

Basic principle



- Using conventional PWM methods a positive high frequency (ω) rotating complex voltage vector is sent to the motor (called the TX or transmitted signal).
- The resulting currents are measured using current sensors / shunt resistors.
- The Clarke Transform is used to transform the 3 motor currents to a rotating complex current vector (the RX or received signal).
- Due to the elliptic V to I transfer of the motor inductors, the complex current vector is also elliptic.
- The additional phase delay θ due to the motor R and L is disregarded in this section.

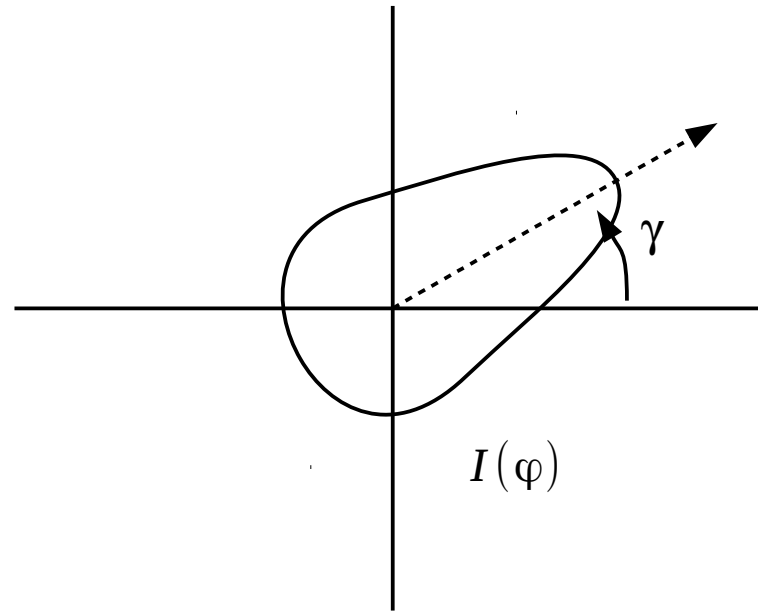
Basic principle



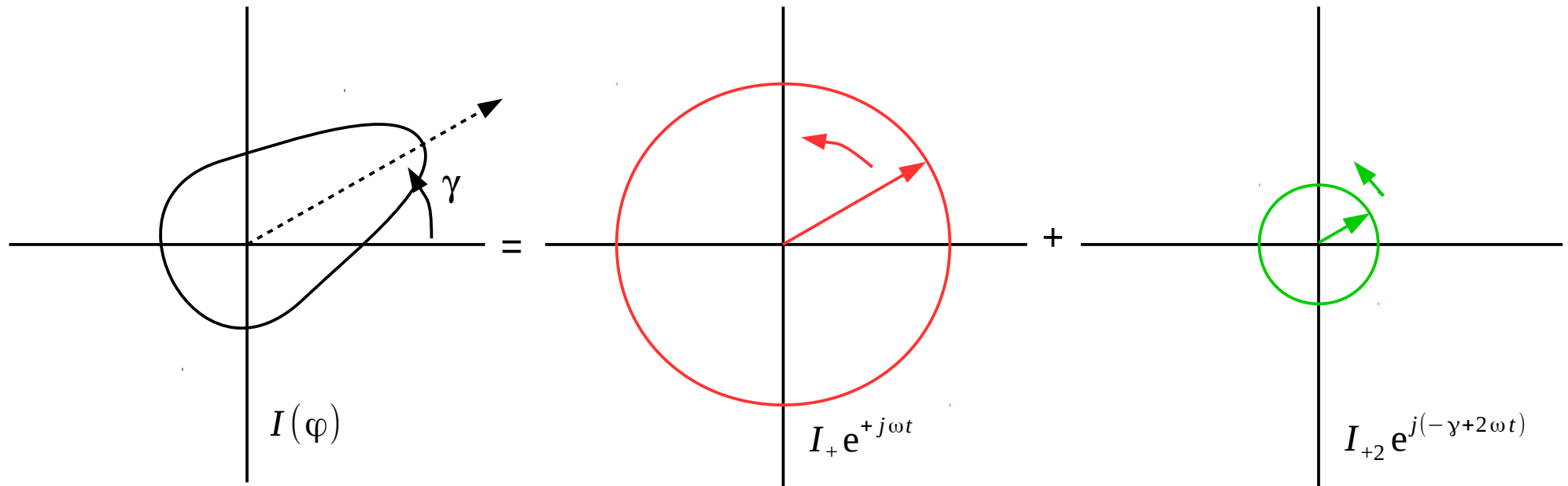
- The elliptic motor current is the sum of a positive and negative direction (frequency) rotating current vector.
- The positive and negative rotating currents have different amplitudes.
- The phase shift in the negative rotating current is indicative of twice the magnetic rotor angle.

Basic principle

The previous slides show how the double angle (2γ) of the rotor magnets can be found by observing the negative fundamental in the current domain. Dividing this angle by 2 gives the alignment of the rotor magnets, but not the polarity. For true phase information the stator currents should have an egg type shape:



Basic principle



An egg shaped current is obtained by adding a positive second harmonic to the fundamental, shifted over $-\gamma$ degrees. To find true phase information, a rotating voltage is send to the motor. The relative phase of the second harmonic in the motor currents indicates the rotor phase.

Basic principle

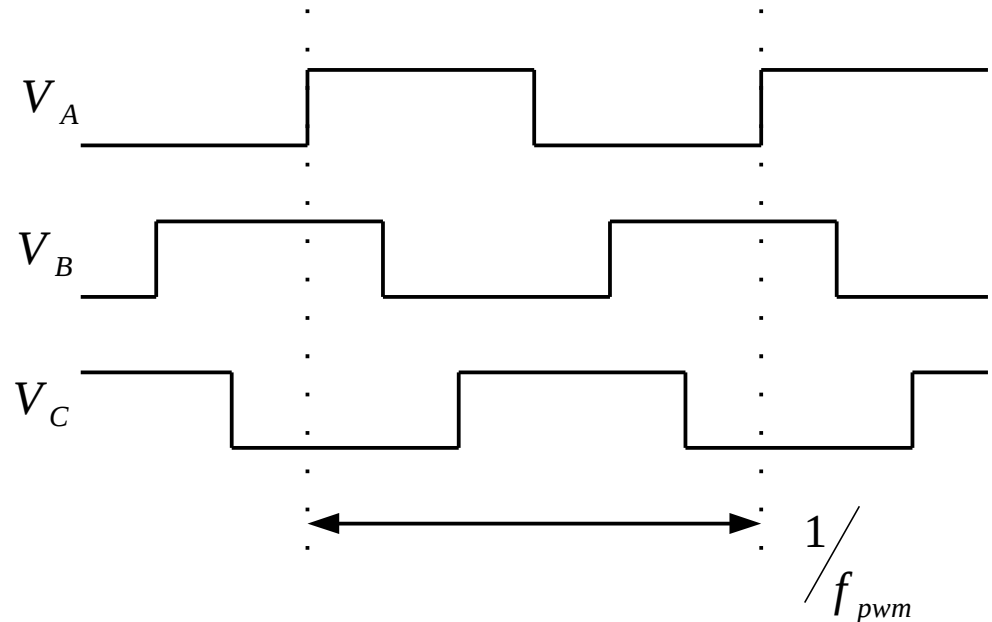
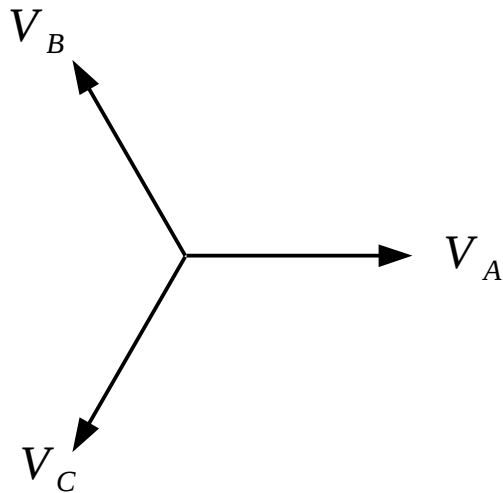
What has been outlined so far is the basic idea, the real world implementation extends this by:

- The rotating voltage signal is actually the PWM signal. The PWM signals are not center aligned but shifted with respect to each other. This generates a rotating voltage signal at the PWM frequency, while still enabling the normal use of the PWM signals for driving the motor. Note that the PWM duty cycle at 0 output signal is 50%.
- The high PWM frequency was chosen for this function because it makes the inductance the dominant source of gain difference in the path from controller output voltage to motor currents.
- Also a high enough PWM frequency is inaudible, making the method silent.
- The method never only sends one rotating voltage signal, but uses 2 or 3 at different frequencies. Consequently it observes 2 or 3 frequencies in the received current signals.
- The method uses the fundamental frequency of the (rectangular) PWM signals, treating them as if they are sine waves.
- The sampling frequency of the main control loop is different from the PWM frequency. This causes folding / aliasing of the PWM signals and makes it possible to process them as if they were generated at a much lower frequency.

Using the PWM frequency

The rotating voltage vector from the previous section is generated at the PWM frequency. For this purpose the PWM signals are not center aligned but shifted with respect to each other.

The most direct option is to shift the signals 120 degrees:

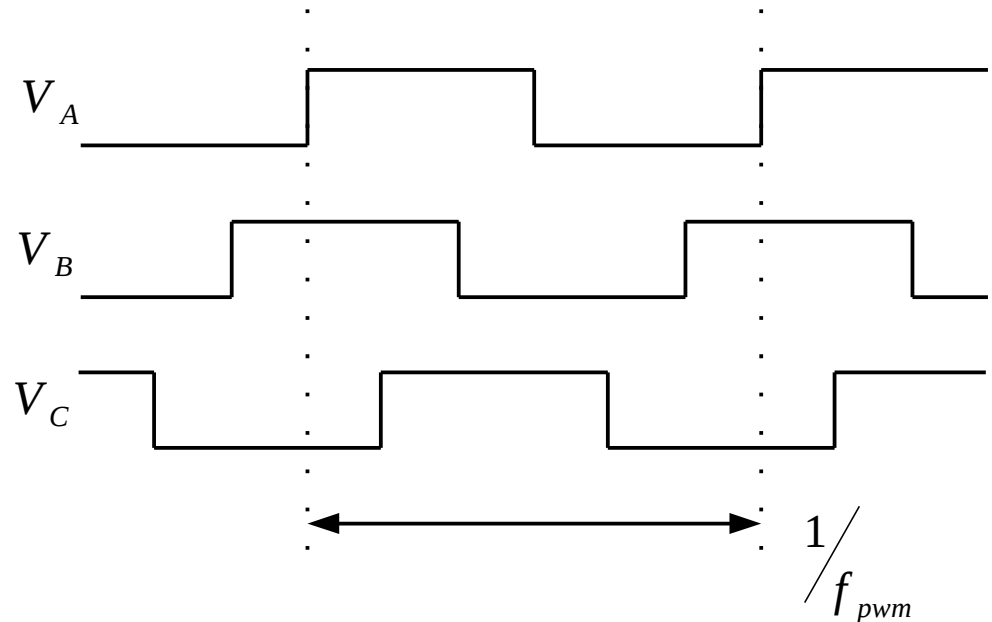
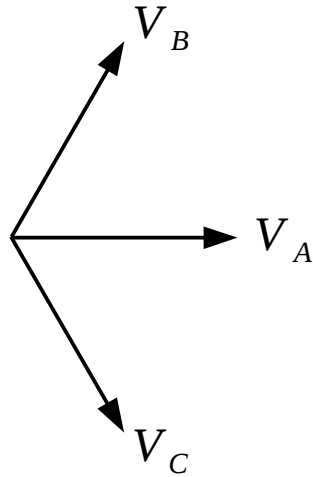


This option was tried and found not to be workable. With a given motor and battery voltage, apart from changing the PWM frequency the current amplitude induced in the motor cannot be influenced. The current will typically be too high.

Using the PWM frequency

For this reason the PWM signals are shifted an arbitrary amount of degrees, such that the current induced is high enough to yield a good S/N ratio at the output of the receiver (appendix B), but are not too high to cause too much unwanted power dissipation.

With a shift of 60 degrees:



This gives good results as far as controllability of the induced current is concerned. The generated signal however is no longer a pure tone at the positive PWM frequency.

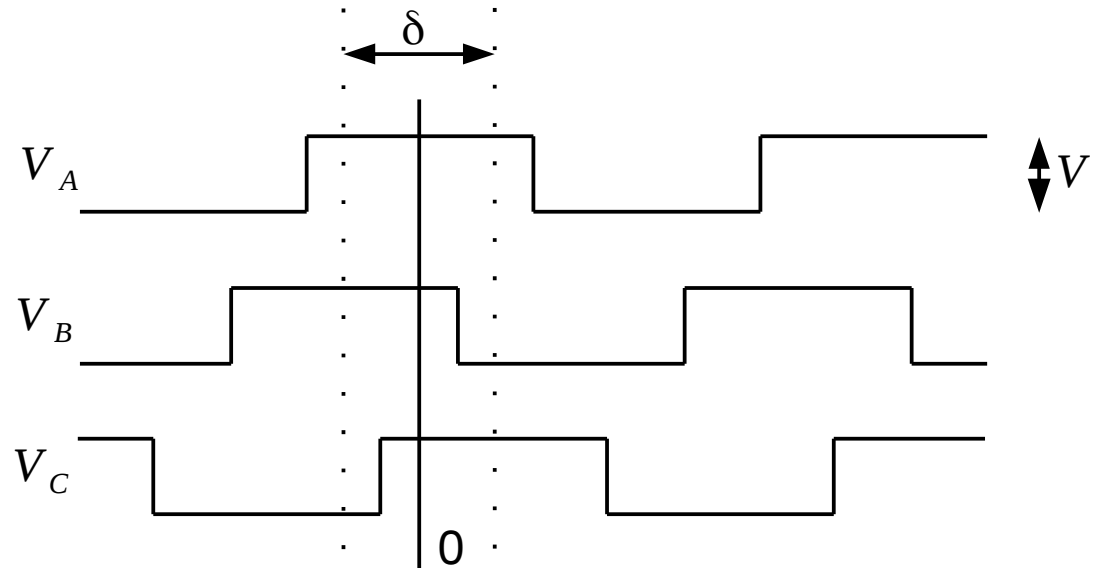
Using the PWM frequency

The frequency content of the generated signal can be calculated using the Clarke transform (Appendix A).

$$V_A = A_A \cos(\omega t)$$

$$V_B = A_B \cos(\omega t + \frac{\delta}{2})$$

$$V_C = A_C \cos(\omega t - \frac{\delta}{2})$$



The amplitudes of the fundamental components A_A , A_B and A_C for a rectangular wave depend on the duty cycle DC:

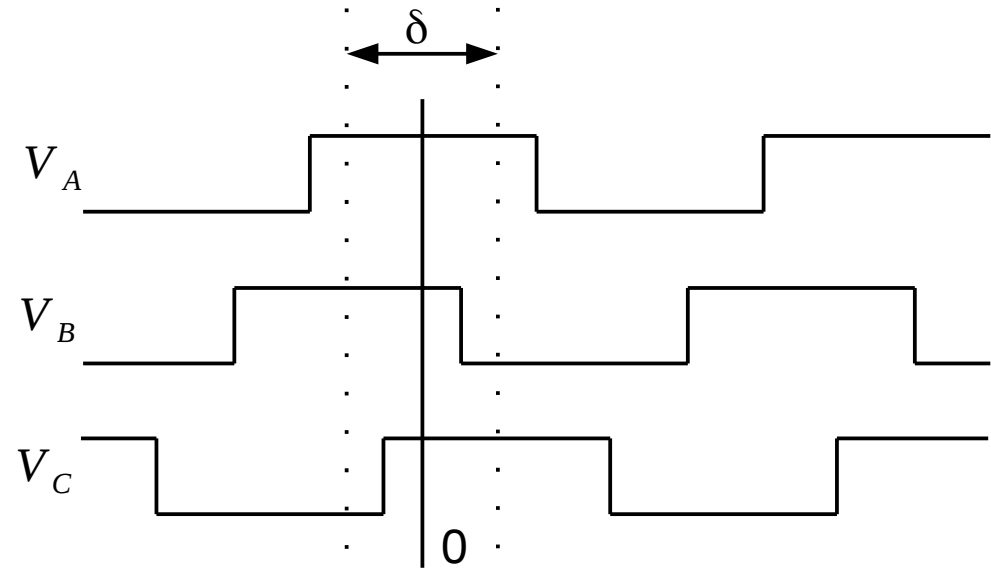
$$A_x = \frac{2V}{\pi} \sin(\pi DC_x)$$

Using the PWM frequency

$$V_A = A_A \cos(\omega t) = \frac{A_A}{2} [e^{j\omega t} + e^{-j\omega t}]$$

$$V_B = A_B \cos(\omega t + \frac{\delta}{2}) = \frac{A_B}{2} [e^{j(\omega t + \frac{\delta}{2})} + e^{-j(\omega t + \frac{\delta}{2})}]$$

$$V_C = A_C \cos(\omega t - \frac{\delta}{2}) = \frac{A_C}{2} [e^{j(\omega t - \frac{\delta}{2})} + e^{-j(\omega t - \frac{\delta}{2})}]$$



Applying the Clarke transform:

$$V_{real} + jV_{imag} = e^{j\omega t} \left[\frac{A_A}{2} + \frac{A_B}{2} e^{j(\frac{\delta}{2} - 2\pi/3)} + \frac{A_C}{2} e^{-j(\frac{\delta}{2} - 2\pi/3)} \right] + e^{-j\omega t} \left[\frac{A_A}{2} + \frac{A_B}{2} e^{j(\frac{\delta}{2} + 2\pi/3)} + \frac{A_C}{2} e^{-j(\frac{\delta}{2} + 2\pi/3)} \right]$$

Using the PWM frequency

$$V_{real} + jV_{imag} = e^{j\omega t} \left[\frac{A_A}{2} + \frac{A_B}{2} e^{j(\frac{\delta}{2} - 2\pi/3)} + \frac{A_C}{2} e^{-j(\frac{\delta}{2} - 2\pi/3)} \right] + e^{-j\omega t} \left[\frac{A_A}{2} + \frac{A_B}{2} e^{j(\frac{\delta}{2} + 2\pi/3)} + \frac{A_C}{2} e^{-j(\frac{\delta}{2} + 2\pi/3)} \right]$$

The transform shows the PWM induced signal has both a positive ($e^{j\omega t}$) and a negative ($e^{-j\omega t}$) frequency component. Dependent on the duty cycles outputted with the PWM channels, the PWM frequency signals may have complex amplitudes (meaning the transmitted signals have a duty cycle dependent phase shift).

For all three amplitudes equal:

$$A = A_A = A_B = A_C$$

$$V_{real} + jV_{imag} = e^{j\omega t} \left[\frac{A}{2} + A \cos\left(\frac{\delta}{2} - 2\pi/3\right) \right] + e^{-j\omega t} \left[\frac{A}{2} + A \cos\left(\frac{\delta}{2} + 2\pi/3\right) \right]$$

In my application $\delta = 2\pi/3$ is a good choice (as this results in a good S/N ratio at the decoded receiver output without causing too much power dissipation), leading to

$$V_{real} + jV_{imag} = A e^{j\omega t} - 0.5 A e^{-j\omega t}$$

Using the PWM frequency

$$V_{real} + jV_{imag} = A e^{j\omega t} - 0.5 A e^{-j\omega t}$$

So once the phase shift between the PWM signals is no longer equal to 120 degrees, or when the amplitudes of the fundamentals are no longer equal, the PWM signals contain both a forward and reverse rotating component.

The negative rotating TX (transmitted) component will be added to the saliency induced negative rotating RX (received) component, and vice versa.

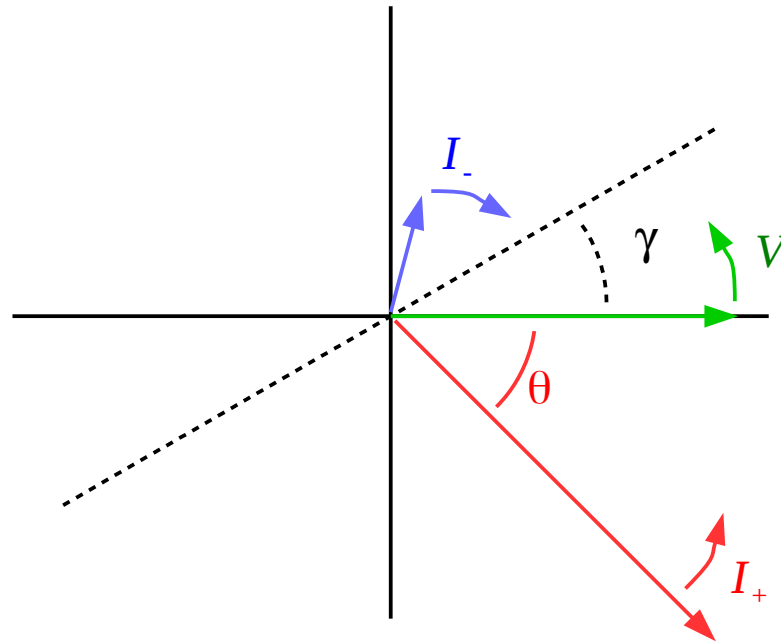
Note for later: for obtaining the positive and negative rotating TX components only 2 channels are necessary. Choosing $A_A=0$ and $A=A_B=A_C$ results in:

$$V_{real} + jV_{imag} = e^{j\omega t} [A \cos(\frac{\delta}{2} - 2\pi/3)] + e^{-j\omega t} [A \cos(\frac{\delta}{2} + 2\pi/3)]$$

With $\delta = 4\pi/3$ this results in

$$V_{real} + jV_{imag} = A e^{j\omega t} - 0.5 A e^{-j\omega t}$$

The Magnetic Circle Vector



To examine the case of TX-ing both a positive and negative rotating signal, first the case of the positive TX signals is examined. The picture shows the positive TX component in green.

$$V = A_+ e^{j\omega t}$$

The positive direction rotating current (in red) is a direct result of the motor impedance Z .

$$I_+ = z A_+ e^{j(\omega t - \theta)}, \text{ with } z e^{-j\theta} \text{ the (unknown) gain and phase delay of the motor impedance, additional analog processing etc.}$$

The Magnetic Circle Vector

The negative rotating current (in blue) is a result of the saliency and rotor position γ .

$$I_- = x A_+ e^{j(-\omega t + \alpha)}$$

The angle α is such that when $\omega t - \theta = \gamma$ also $-\omega t + \alpha = \gamma$ (as I_+ and I_- overlap at angle γ to form the elliptic shape as discussed earlier). This leads to:

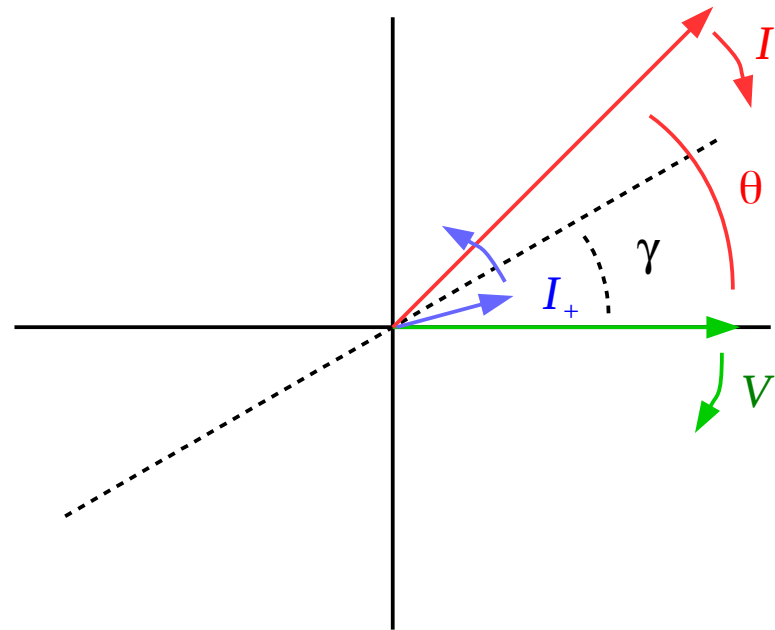
$$I_- = x A_+ e^{j(-\omega t + 2\gamma + \theta)}$$

Here $x e^{j(2\gamma + \theta)}$ can be seen as the transfer function from positive rotating voltage to negative rotating current.

The total current caused by the positive rotating voltage:

$$I = z A_+ e^{j(\omega t - \theta)} + x A_+ e^{j(-\omega t + 2\gamma + \theta)}$$

The Magnetic Circle Vector



The same considerations can be made for the negative direction rotating voltage vector.

$$V = A_- e^{-j\omega t}$$

The resulting current contribution:

$$I = z A_- e^{j(-\omega t + \theta)} + x A_- e^{j(\omega t + 2\gamma - \theta)}$$

The Magnetic Circle Vector

The motor current is the sum of the positive and negative contributions:

$$I = e^{-j\omega t} (z A_- e^{j\theta} + x A_+ e^{j(2\gamma+\theta)}) + e^{j\omega t} (z A_+ e^{-j\theta} + x A_- e^{j(2\gamma-\theta)}) + I_{\text{power}}$$

This equation only contains one variable of interest, the rotor angle γ . As the amplitude of the complex numbers does not matter, therefore many of the following equations will use the operator \propto (proportional to) instead of $=$ (equal to).

Two receiver structures can be used to split the motor current into its $e^{-j\omega t}$ and $e^{j\omega t}$ components. The receivers share the same hardware and code up to the output of the Clarke transform. The two receiver output signals:

$$PQ_+ = p_+ + jq_+ \propto z k e^{j\theta} + x e^{j2\gamma+j\theta} \quad \text{with } k = \frac{A_-}{A_+}$$

$$PQ_- = p_- + jq_- \propto z e^{-j\theta} + x k e^{j2\gamma-j\theta}$$

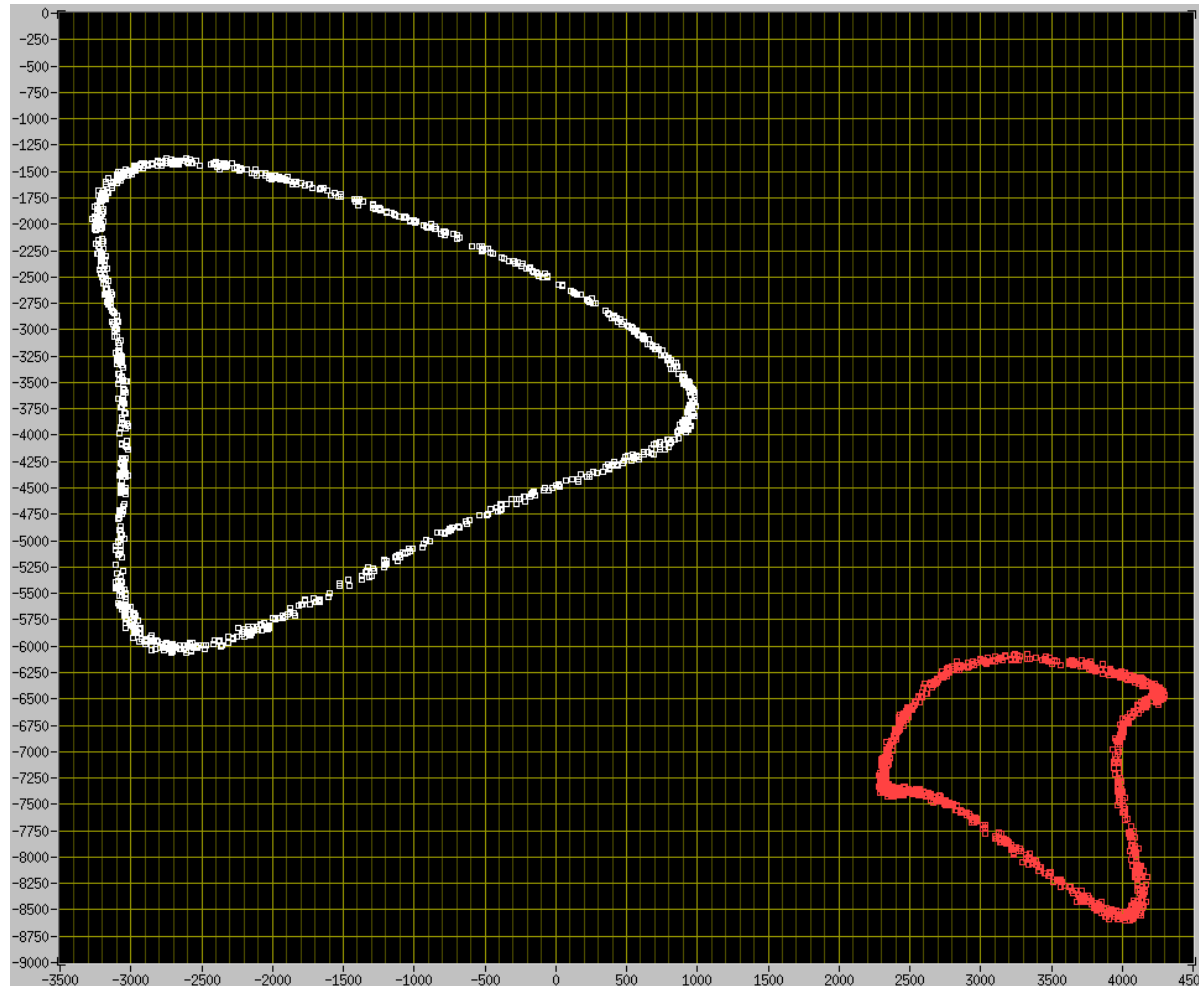
Recalling the TX signal $V_{\text{real}} + jV_{\text{imag}} = A e^{j\omega t} - 0.5 A e^{-j\omega t}$, meaning here $k = \frac{-0.5 A}{A} = -0.5$

The Magnetic Circle Vector



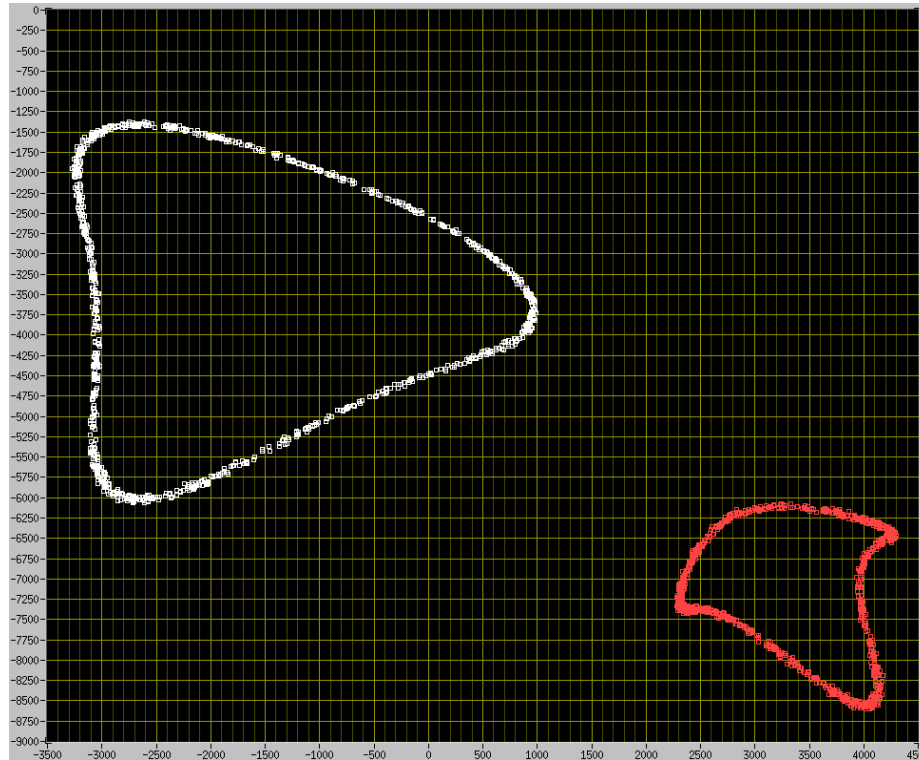
The above pictures shows the PQ_+ (white) and PQ_- (red) vectors in the complex plane, for a motor standing still. Due to noise plotting multiple points results in small blobs instead of single points.

The Magnetic Circle Vector



When the motor is rotated the shape of the $x e^{j2\gamma}$ rotor position component becomes visible. For the motor used the saliency is not constant, resulting in the shapes as shown. Other motors tested have shown constant saliency, resulting in more circular shapes. The size of the shapes (compared to the distance to the origin) depends on the amount of saliency.

The Magnetic Circle Vector



Note how the shapes show the properties of the TX signal. The red PQ_- shape shows a large offset (from the origin) due to the large positive frequency TX signal, but the small saliency signal coming from the smaller negative TX signal. For the white PQ_+ shape, it shows the smaller negative TX signal and the larger saliency signal caused by the large positive TX signal.

Guesstimating the centers of the shapes and determining the vector lengths, combined with realizing that the white shape is mirrored in the origin, shows the k value of -0.5 .

The Magnetic Circle Vector

To find $e^{j2\gamma}$ the equation for PQ_+ is multiplied by $k e^{-j\theta}$. The complex conjugate ($*$) of the equation for PQ_- is multiplied by $e^{-j\theta}$. This yields

$$\begin{aligned}zk^2 + xk e^{j2\gamma} &= kPQ_+ e^{-j\theta} \\z + xk e^{-j2\gamma} &= PQ_-^* e^{-j\theta}\end{aligned}$$

Adding together:

$$z(k^2+1) + 2xk \cos(2\gamma) = e^{-j\theta}(kPQ_+ + PQ_-^*)$$

Real when both TX signals A_+ and A_- are real.

then this side of the equation must be real


$$e^{j\theta} \propto kPQ_+ + PQ_-^*$$

This eliminates the need to know or measure the phase delay θ of the motor impedance and analog signal processing filters (LNA).

The Magnetic Circle Vector

Eliminating $e^{j\theta}$ and z yields

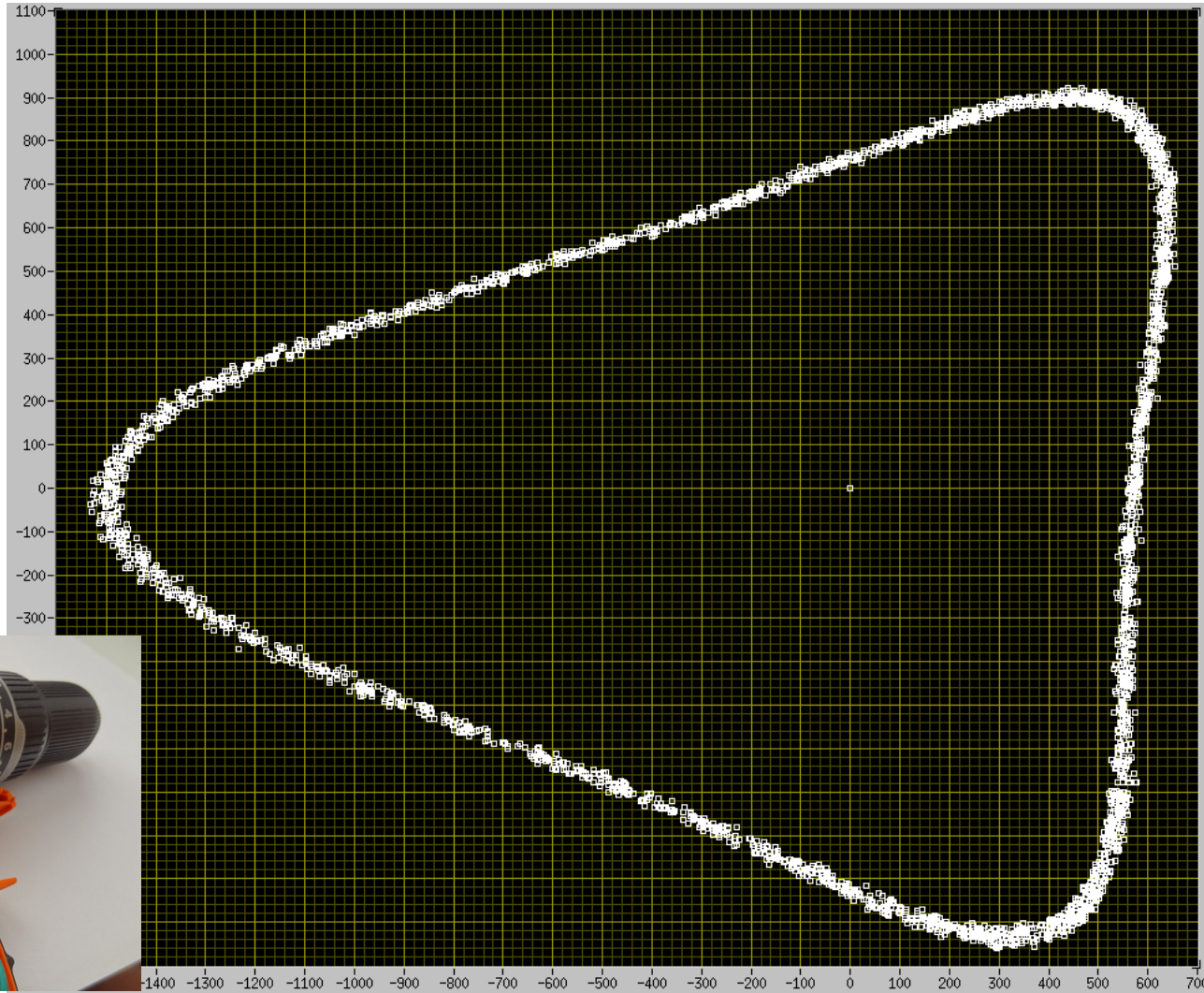
$$e^{j2\gamma} \propto PQ_+ PQ_- + \frac{k}{(1-k^2)} (|PQ_+|^2 - |PQ_-|^2)$$

A for coding more convenient version, valid under the condition that $(1-k^2) > 0$:

$$e^{j2\gamma} \propto (1-k^2) PQ_+ PQ_- + k (|PQ_+|^2 - |PQ_-|^2)$$

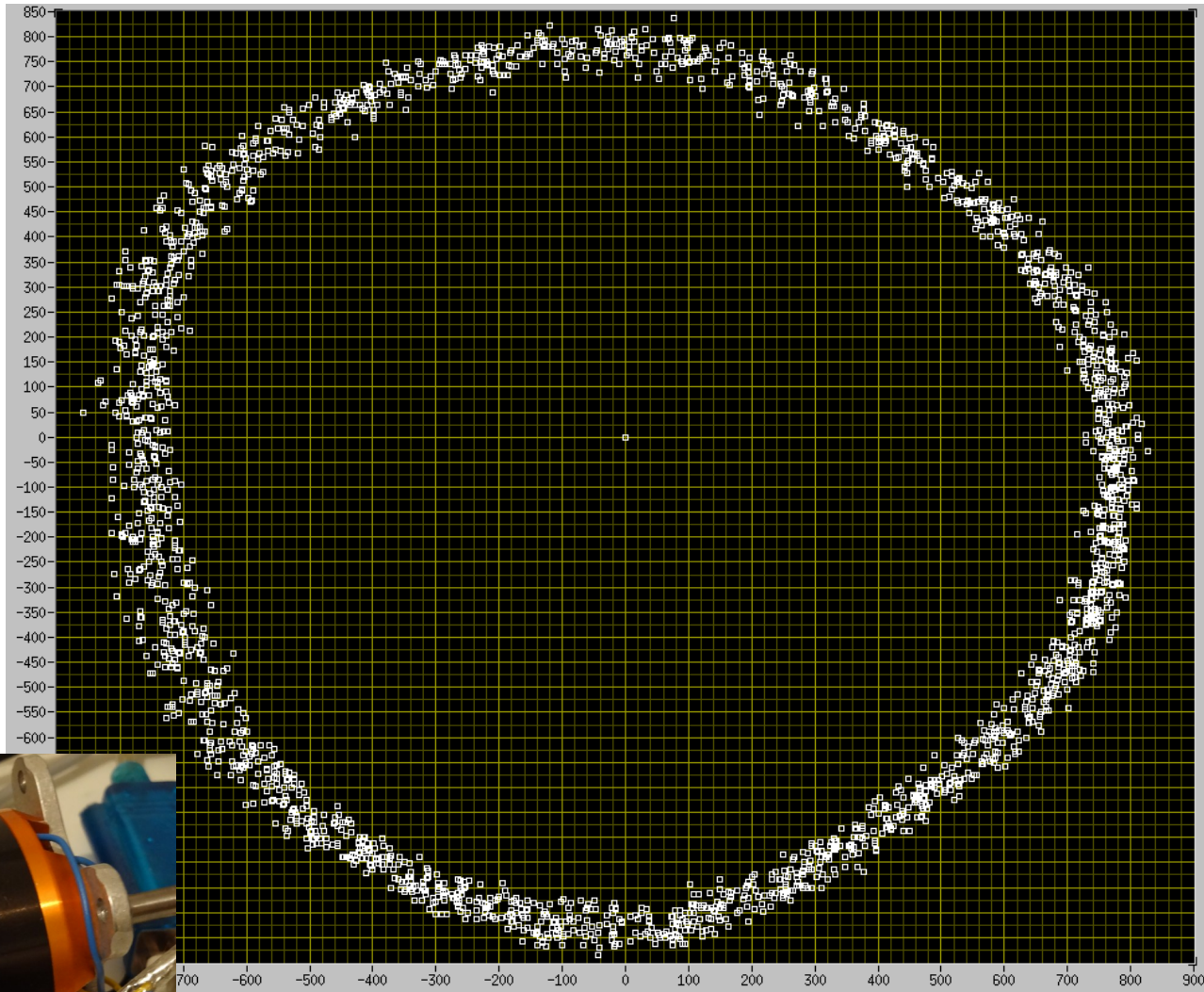
Looking at the equation, the first term is a complex circle, the second term a shift along the real axis. All variables to do with the transfer functions from TX signal to RX signal are eliminated, to find $e^{j2\gamma}$ one only needs the received signals and the known TX signal properties captured in the variable k . **This means no calibration, precisely known external signal processing (LNA) or initial full motor rotation is necessary.**

The Magnetic Circle Vector



The figure above shows the Magnetic Circle Vector ($e^{j2\gamma}$) as calculated for a running (drill) motor, using the previously shown PQ_+ and PQ_- signals.

The Magnetic Circle Vector



This is the much more circular MCV for a running small Remote Control model airplane motor (rewound with only 4 windings per tooth) .

The Magnetic Circle Vector

Properties of the MCV:

- The shape of the MCV is motor dependent, as with the PQ signals.
- The Signal to Noise ratio of the entire signal path determines the 'fuzziness' of the MCV, and thus the noise on $e^{j2\gamma}$. A larger TX signal increases the received signal, but takes more current from the battery. Noise can be reduced by using lower bandwidth filtering in the receiver, but this limits the max motor speed at which this algorithm can be used. Current sensors better matched to the motor will give more signal (at a constant noise contribution), improving the S/N ratio.
- As motor speed increases the filtering in the RX path makes the MCV smaller and more circular (mainly due to the last filter in the RX path).
- Gain mismatch between the motor current sensors and paths in the LNA cause the origin not to be perfectly centered in the MCV. This affects the accuracy of the CORDIC when extracting 2γ from $e^{j2\gamma}$.
- The derivation of the equation for $e^{j2\gamma}$ assumes the TX signals A_+ and A_- to be real. As the motor driving voltage changes the output duty cycles, the three PWM fundamental amplitudes A_A, A_B and A_C change, affecting A_+ and A_- . Dependent on the changeover point to back-emf standard sensorless FOC and the required accuracy of the phase information, the TX signal must be actively controlled to keep A_+ and A_- real (see appendix C).

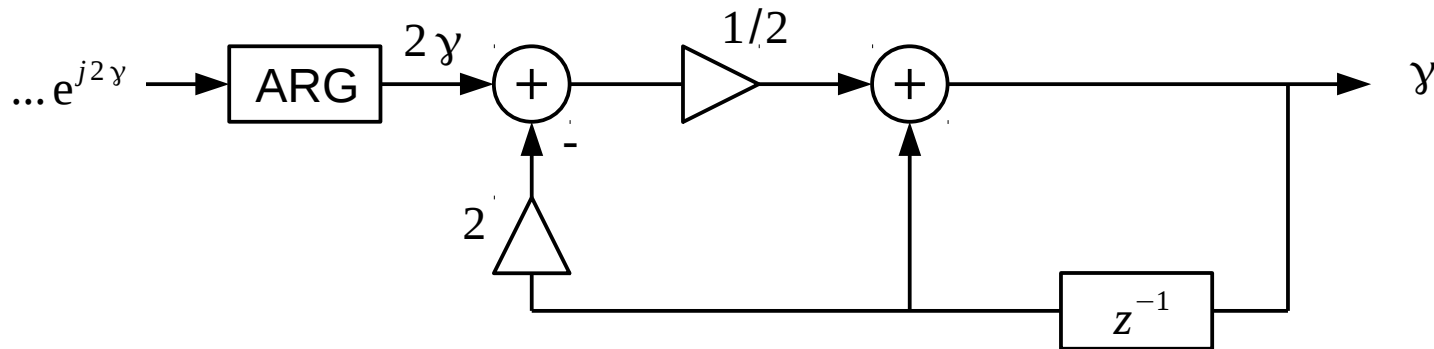
The Magnetic Circle Vector

Properties of the MCV:

- A different equation for $e^{j2\gamma}$ can be probably derived allowing the use of non-real A_+ and A_- . This has not been done yet.
- For the MCV it does not matter whether 2 or 3 of the PWM outputs are involved with generating A_+ and A_- .
- The MCV does not distinguish between saliency caused by field coming from the rotor permanent magnets, field coming from the stator coils and saliency caused by inherent Switched Reluctance behavior (as in an IPM motor). This must be taken into account when using the phase information for motor control !
- The shape of the MCV for the drill motor has three extremes at 60, 180 and 300 degrees. This might be typical for a delta connected motor. Keeping in mind the factor 2 in $e^{j2\gamma}$ the shape shows maximum signal and therefore minimum inductance at 30, 90 and 150 degrees (and also at -150, -90 and -30 degrees). This corresponds to how the windings are aligned in a delta connected motor. The winding between node A and B for instance is placed at a -30 or 150 degree angle. The small RC motor was star connected.
- The full circumference of the MCV 'corresponds' to the magnet-to-magnet distance of the motor. For the small RC motor this is 9mm. Movements much small than a millimeter can easily be detected !

The Magnetic Circle Vector

The MCV provides 2γ with no offset. Dividing this by 2 means that we get correct 0-179 degree phase info, but we do not know whether to add 0 or 180 to this to arrive at the absolute rotor phase. With the phase info being 16 bit, this comes down to the MSB being unknown. A structure for dividing 2γ by 2 is used that ensures correct roll-over to the 0 / 180 MSB bit, such that we only need to add a constant 0 or 180 degree offset to arrive at absolute rotor phase.



With z^{-1} a unit delay.

With the correct roll-over taken care of, whether to add a constant value of 0 or 180 to γ (invert the MSB or not ?) must be determined next.

Determining the MSB

At this point the phase of the rotor magnets is known, but not their polarity (in case of a Switched Reluctance motor we would be done now). Several measurement options were considered:

- Apply a torque producing current and observe motor rotation.
 - This needs motor movement and is therefore not a true 'from standstill at power up' solution.
 - The rotor might be moving (in the opposite direction) due to an external force larger than the torque from the motor current, and therefore lead to a wrong conclusion.
- Add a field increasing / decreasing current ('blind' or 'imaginary' current) and observe the radius of the MCV.
- Divide the already present rotating measurement current into two camps, observe the MCV for both and draw conclusions from this.

The last two methods both make use of the method for obtaining the MCV being unable to distinguish between rotor and coil-induced magnetic fields. They were considered until it was realized that both make use of second order distortion. Remember that, see the first few slides, the egg-shaped induced current (giving absolute phase info) is also the result of the same second order distortion effect.

Determining the MSB

A common and effective way of measuring the second order distortion is to apply two tones and observe their frequency-sum or -difference component. The second order effect in the motor is described by

$$y = \alpha e^{-j\xi} x^2$$

Here we are interested in ξ , as it provides 0-359 degree info about the rotor position. Using a dual tone signal

$$x = A_1 e^{j\omega_1 t} + A_2 e^{j\omega_2 t}$$

results in

$$y = \alpha e^{-j\xi} [A_1^2 e^{j2\omega_1 t} + A_2^2 e^{j2\omega_2 t} + 2A_1 A_2 e^{j(\omega_1 + \omega_2)t}]$$

The dual frequency components $2\omega_1$ and $2\omega_2$ in the RX signal are heavily polluted by the second harmonic components of the motor-powering TX signals. Therefore here the sum frequency $\omega_1 + \omega_2$ is observed (by a receiver structure) to obtain ξ .

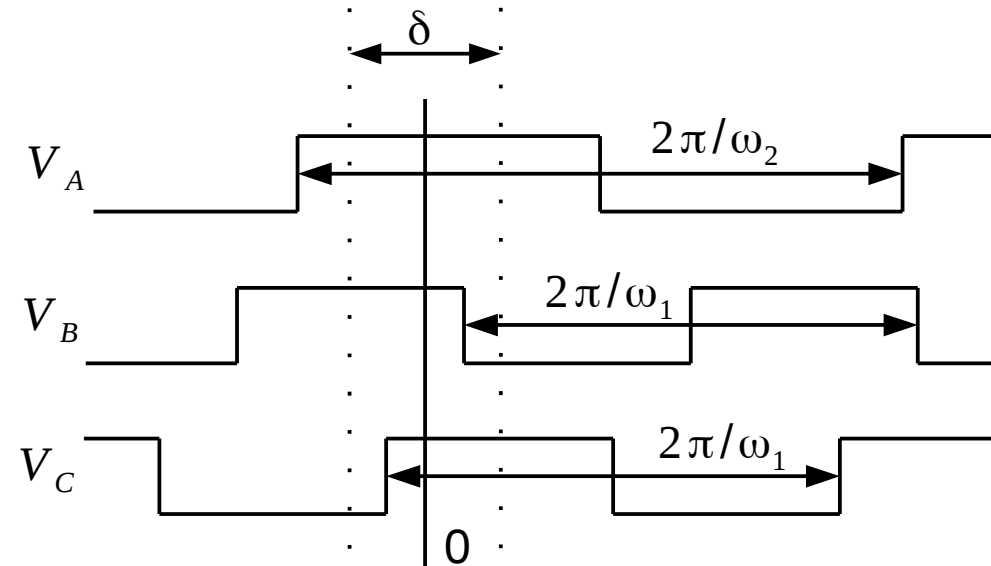
Determining the MSB

Again the PWM signals are used to generate the TX signals. Two channels (here B and C) are used for ω_1 , one channel (A) for ω_2 .

$$V_A = A_A \cos(\omega_2 t) = \frac{A_A}{2} [e^{j\omega_2 t} + e^{-j\omega_2 t}]$$

$$V_B = A_B \cos\left(\omega_1 t + \frac{\delta}{2}\right) = \frac{A_B}{2} [e^{j(\omega_1 t + \frac{\delta}{2})} + e^{-j(\omega_1 t + \frac{\delta}{2})}]$$

$$V_C = A_C \cos\left(\omega_1 t - \frac{\delta}{2}\right) = \frac{A_C}{2} [e^{j(\omega_1 t - \frac{\delta}{2})} + e^{-j(\omega_1 t - \frac{\delta}{2})}]$$



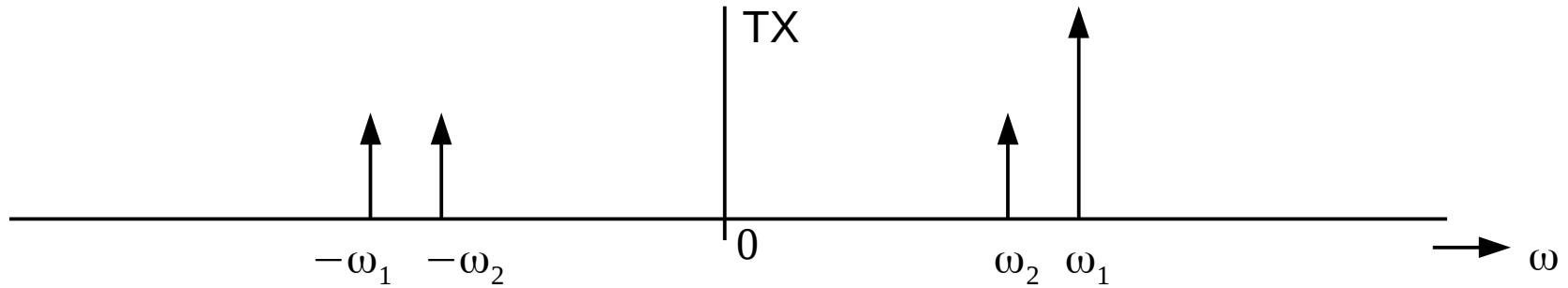
Applying the Clarke transform:

$$V_{real} + jV_{imag} = e^{j\omega_2 t} \frac{A_A}{2} + e^{-j\omega_2 t} \frac{A_A}{2} + e^{j\omega_1 t} \left[\frac{A_B}{2} e^{j(\frac{\delta}{2} - 2\pi/3)} + \frac{A_C}{2} e^{-j(\frac{\delta}{2} - 2\pi/3)} \right] + e^{-j\omega_1 t} \left[\frac{A_B}{2} e^{j(\frac{\delta}{2} + 2\pi/3)} + \frac{A_C}{2} e^{-j(\frac{\delta}{2} + 2\pi/3)} \right]$$

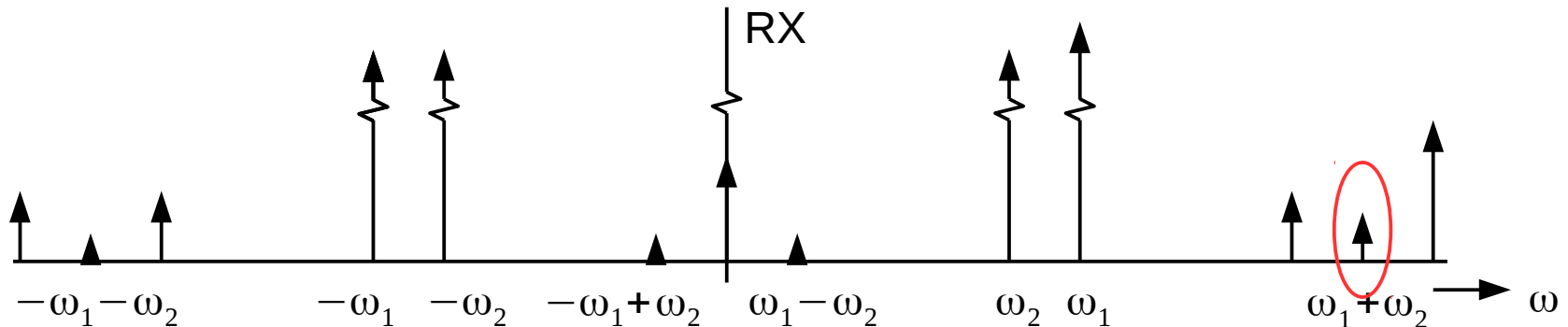
Determining the MSB

Choosing $A = A_A = A_B = A_C$ and $\delta = 4\pi/3$ results in:

$$V_{real} + jV_{imag} = 0.5Ae^{j\omega_2 t} + 0.5Ae^{-j\omega_2 t} + Ae^{j\omega_1 t} - 0.5Ae^{-j\omega_1 t}$$



Passing this TX signal through the saliency induced non-linear motor results in a RX signal with many extra frequency components. The different amplitudes in the TX signal make that the component at $\omega_1 + \omega_2$ is the largest component caused by the second order non-linearity.



Determining the MSB

The second order effect as discussed here is very weak. Its amplitude in the RX signal can be increased by increasing both ω_1 and ω_2 components. Component ω_1 can be influenced by frequency ω_1 and phase offset δ . The amplitude of component ω_2 can only be influenced by changing its frequency.

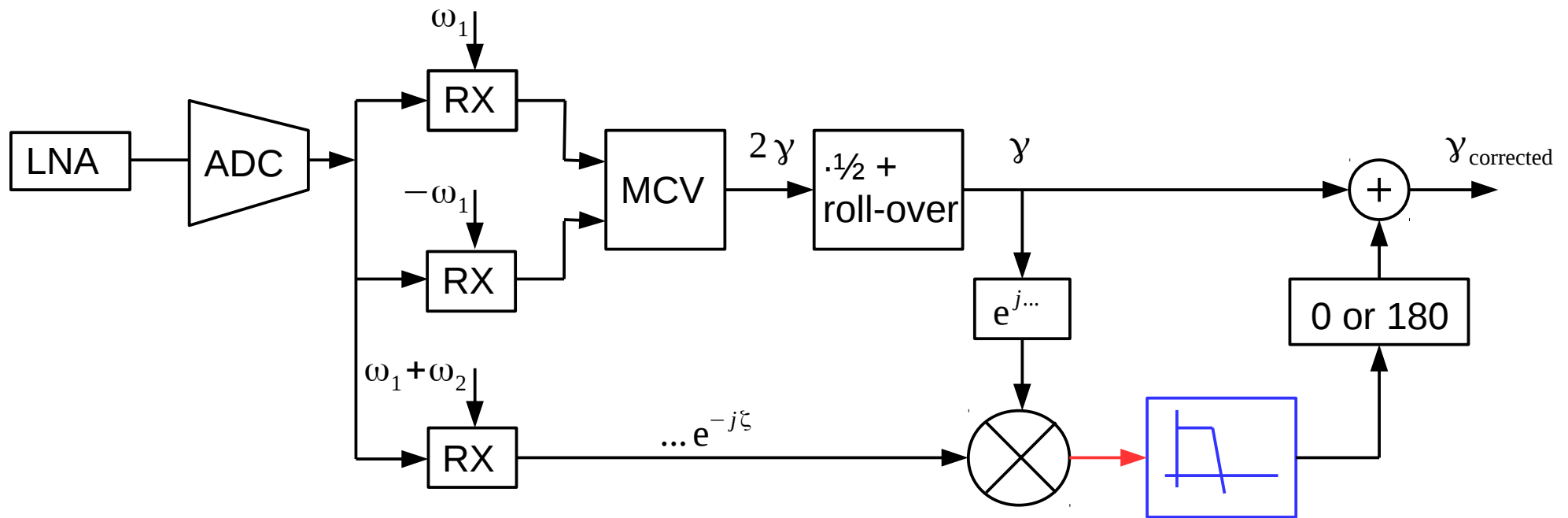
Even then the resulting $\omega_1 + \omega_2$ component in the RX signal is very weak. To get a reliable (low noise) signal at the output of the receiver a very narrow filter is necessary. The narrow filter means the signal is only present for very low rotor speeds, at higher speeds it will be removed by the RX filter.

But, we only need the second order component one time to determine the rotor phase MSB, as discussed earlier. Once determined the MCV combined with proper MSB roll-over can be used to keep track of the rotor phase and the second order component is no longer necessary.

For instance, two PWM frequencies and the second order effect can be used at a cold startup to determine the absolute rotor phase. Once determined a switch-over is made to only one PWM frequency. The MCV with correct MSB roll-over is then used to keep track of absolute rotor phase.

Another method for applying two tones: use the shifted PWM signals for one tone and Phase Modulation (appendix D) for the second tone. Then sector switching (as discussed in the next slides) is probably not necessary.

Determining the MSB

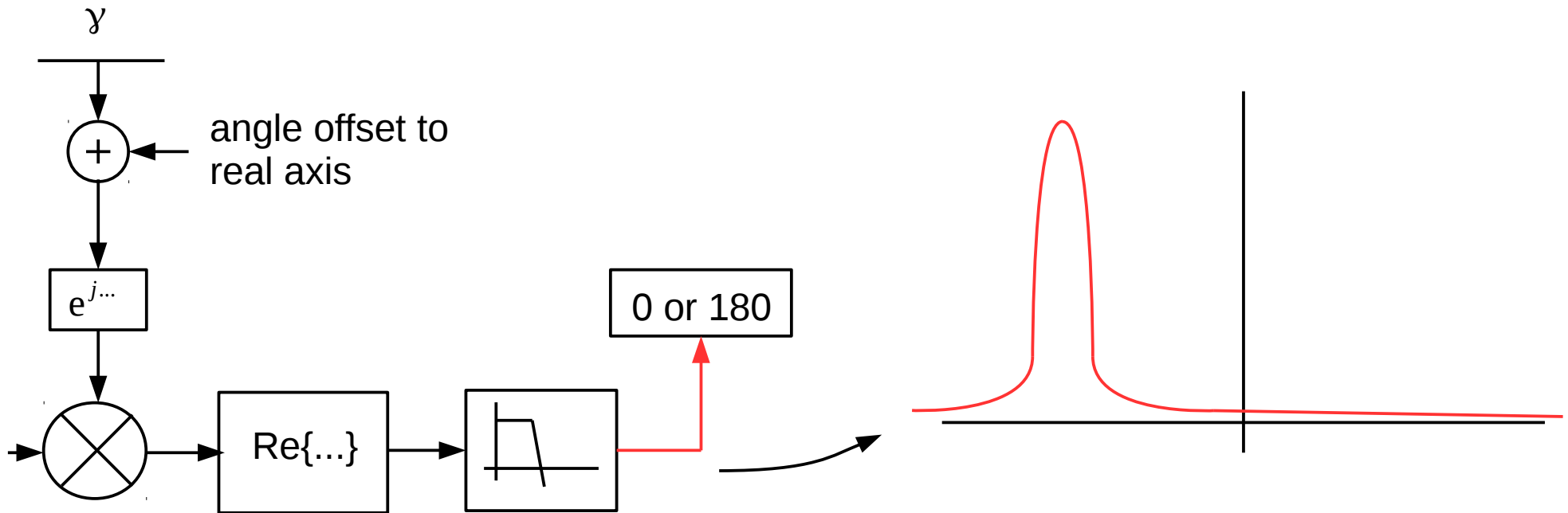


The above structure is used to determine the MSB and arrive at $\gamma_{corrected}$.

Two RX structures are used to find the MCV, determine 2γ and divide by 2 (with roll-over) to arrive at γ . A separate RX structure (which might have its own LNA and ADCs) is used to find the absolute rotor phase vector $\dots e^{-j\xi}$. Rotating this vector over γ (the resulting signal is indicated in red) will result in one of only two possible **constant and independent of rotor movement** vector angles (or: either one of two possible vectors), one for 0 degree offset in γ and the other one for 180 degree offset in γ . This depends on startup conditions.

As the signal indicated in red does not rotate, the (blue) filter can be very low bandwidth !

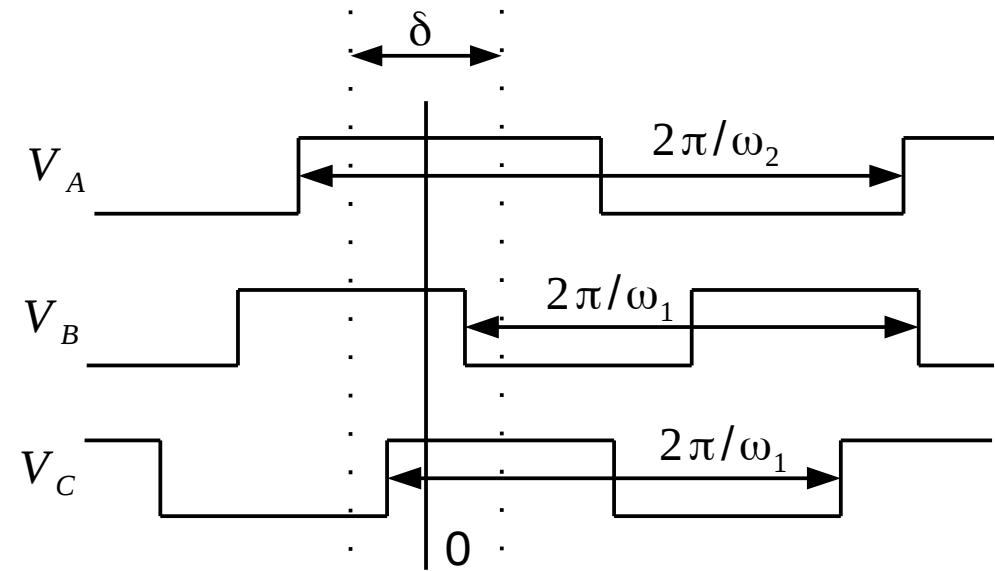
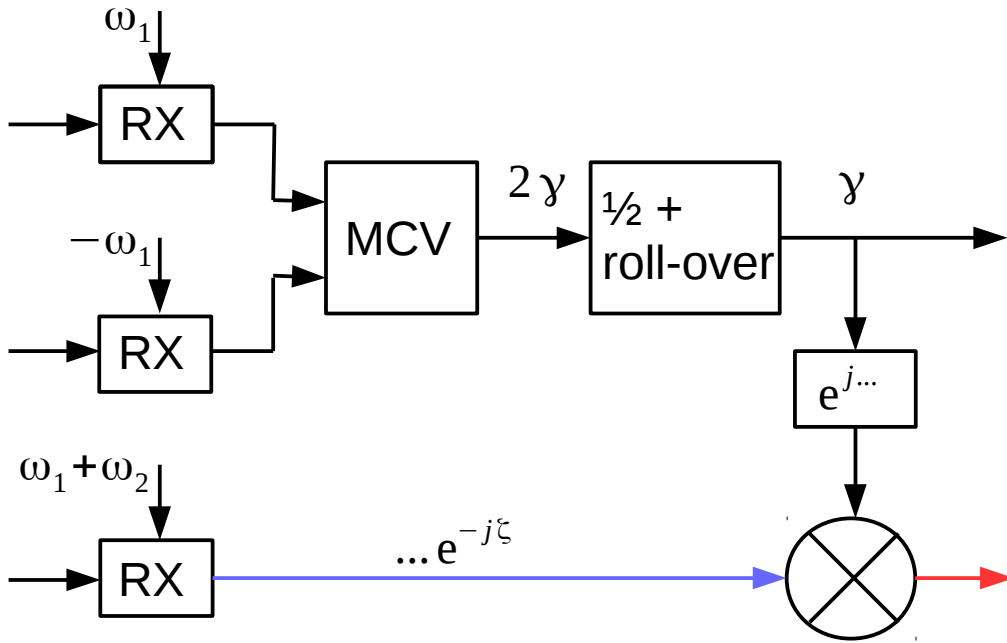
Determining the MSB



Adding an offset to γ will rotate the two possible vectors to the Real axis. Then only one filter is necessary to derive the signal (red) on which the 0 / 180 degree decision is based. Due to the (after filtering) remaining noise the red signal has a distribution as shown above. The larger the S/N ratio of this signal, the higher the chance of a correct 0 / 180 degree decision. Reducing the filter bandwidth reduces the variance of the distribution (noise), but increases the necessary filter response time. In the drill demo the measurement time is 70 msec.

An additional comparator is used to detect a 0 crossing of the red signal during the measurement. When this happens the process of determining the MSB is reset and restarted.

Sector switching



To see the discussed mechanism in action plots were made of signals $\dots e^{-j\zeta}$ (the blue signal in the above diagram) and $\dots e^{-j(\zeta-\gamma)}$ (the red signal in the diagram). Motor phases B and C were at the same PWM frequency ω_1 , while phase A used the different PWM frequency ω_2 .

Sector switching



Signal $\dots e^{-j\xi}$ (blue in the previous slide) is here shown in white, $\dots e^{-j(\xi-\gamma)}$ is shown in red (also red in the previous slide). The motor was rotated over a bit more than one full e-revolution.

Sector switching



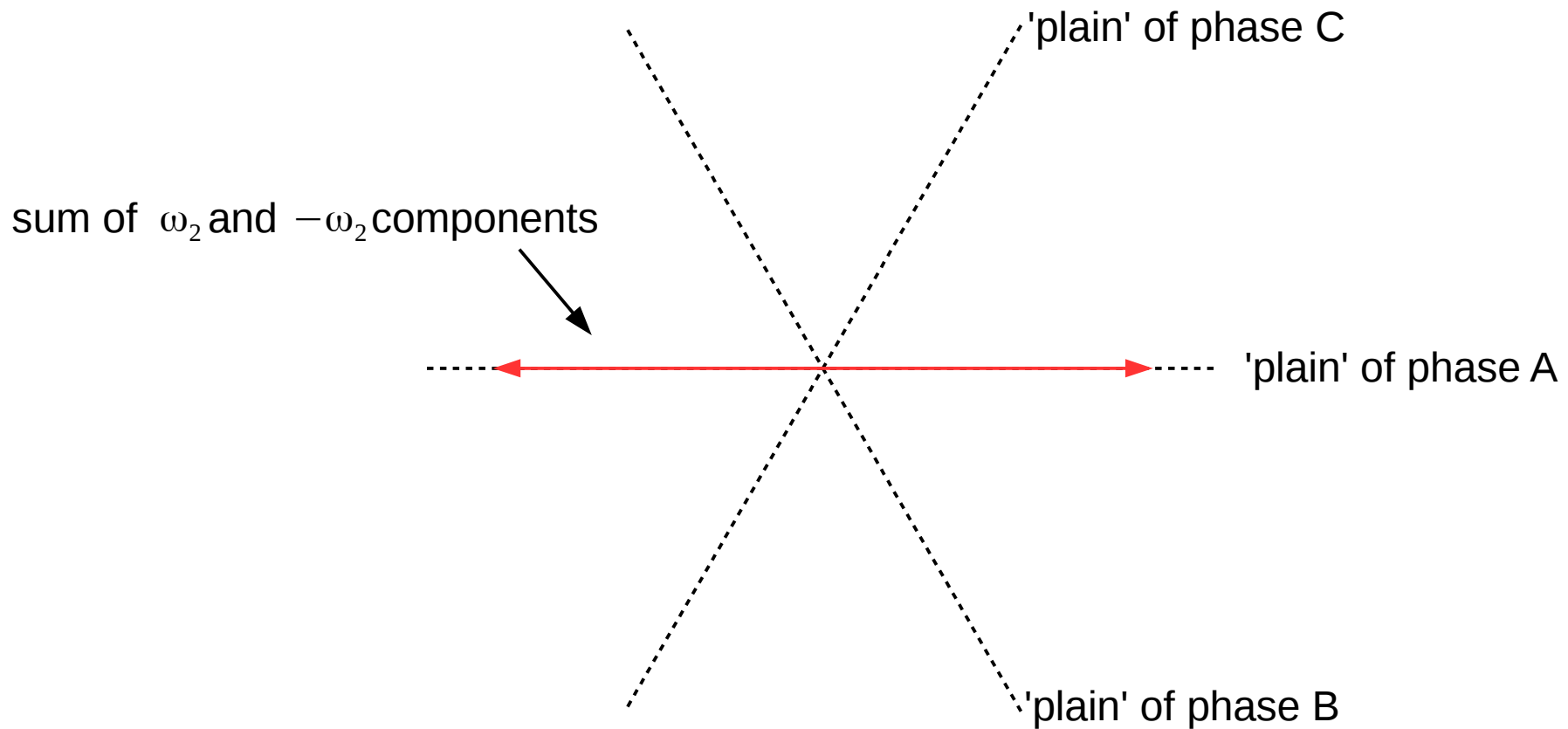
The shape of the figures strongly depends on the motor used (this was with a small RC motor). While the white curve is centered around the origin, the red curve is clearly centered around $-400+50j$. Had the controller started up differently it might have been centered around the opposite point ($400 - 50j$).

Sector switching



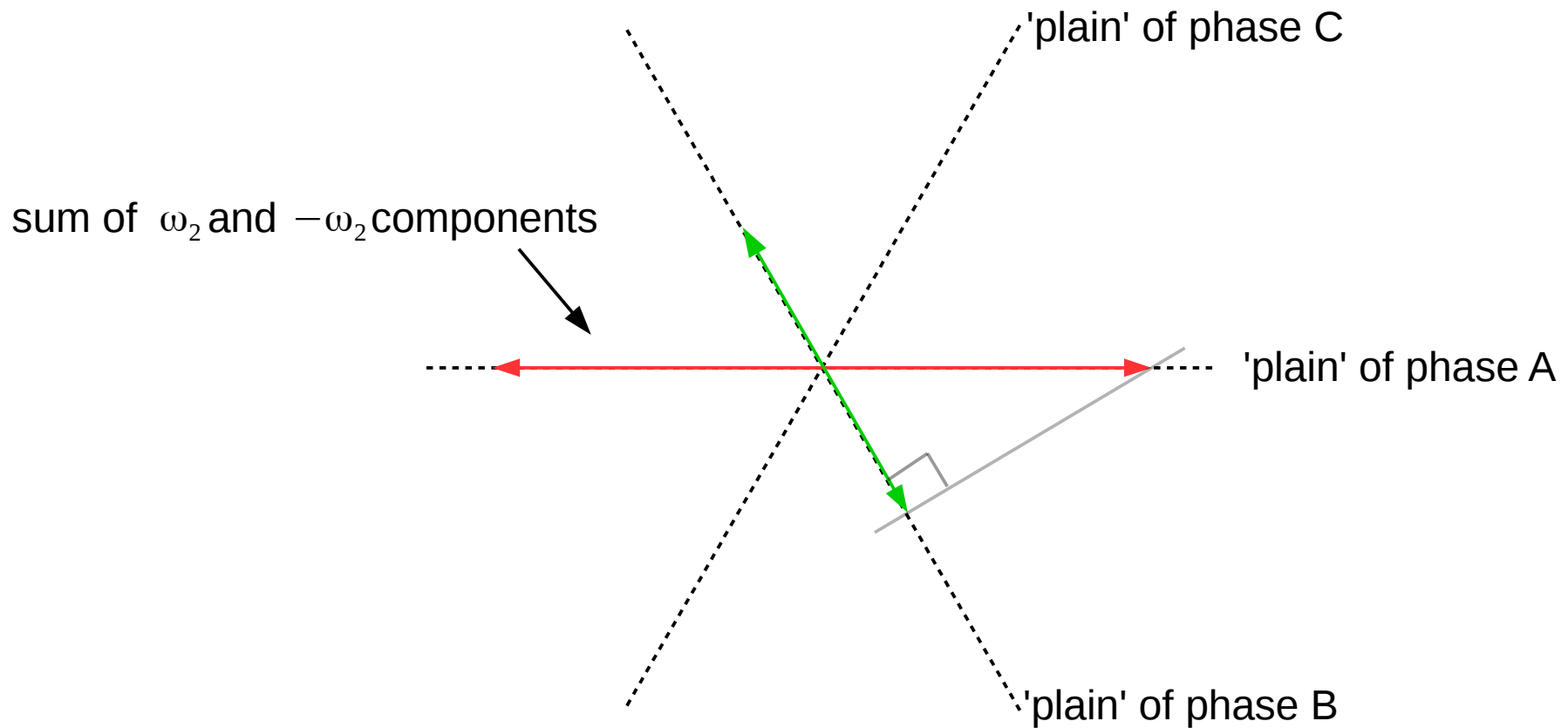
What is also clearly visible is that parts of the white curve (yellow areas) are very close to the origin. Rotated over γ these result in the red curve parts close to the origin. This is a problem as noise on the red curve can cause a wrong MSB decision (see the Gaussian curve of a few slides ago).

Sector switching



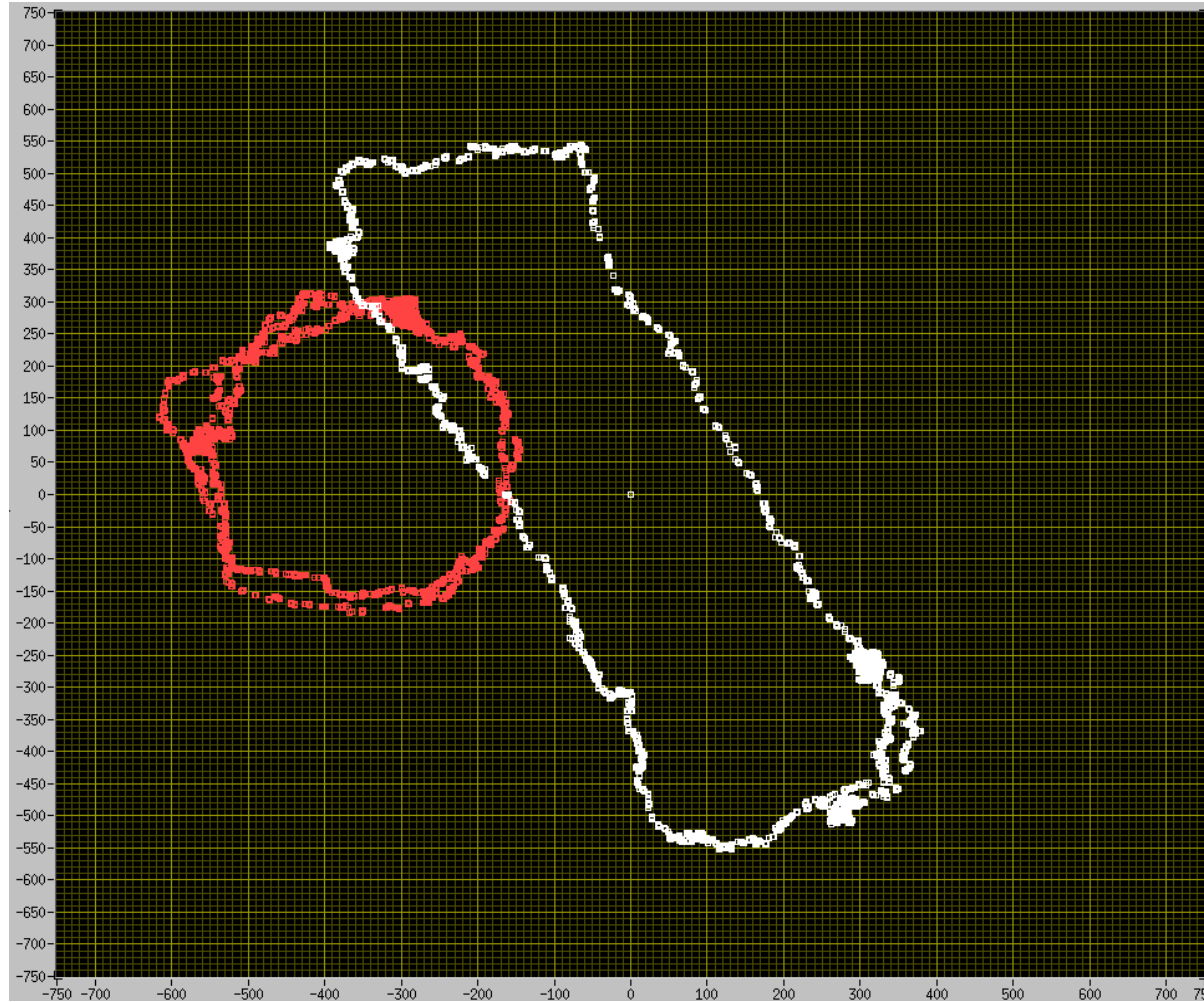
The rectangular shape of the white curve in the previous slide is caused by the different voltage signals supplied to the motor phases. Here phase A runs on the different frequency ω_2 from phases B and C. As the Clarke transform shows, the sum of the ω_2 and $-\omega_2$ components is a vector moving only in the 'plain' of phase A.

Sector switching



While phase A sees the full amplitude of the second frequency, phases B and C only see half ($\cos 60$). Differences in effective amplitudes cause different non-linear responses in the three motor inductors, causing the observed rectangular shape.

Sector switching



Here the second frequency was applied to phase B, with A and C receiving phase shifted versions of frequency 1.

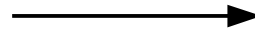
Sector switching



And here the second frequency was applied to phase C, with A and B receiving phase shifted versions of frequency 1.

Note that the startup condition was different from the previous 2 cases, the red curve has rotated over 180 degrees.

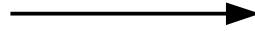
Sector switching



after rotor
rotation
over -60
degrees



phase A: ω_2
phases B, C: ω_1

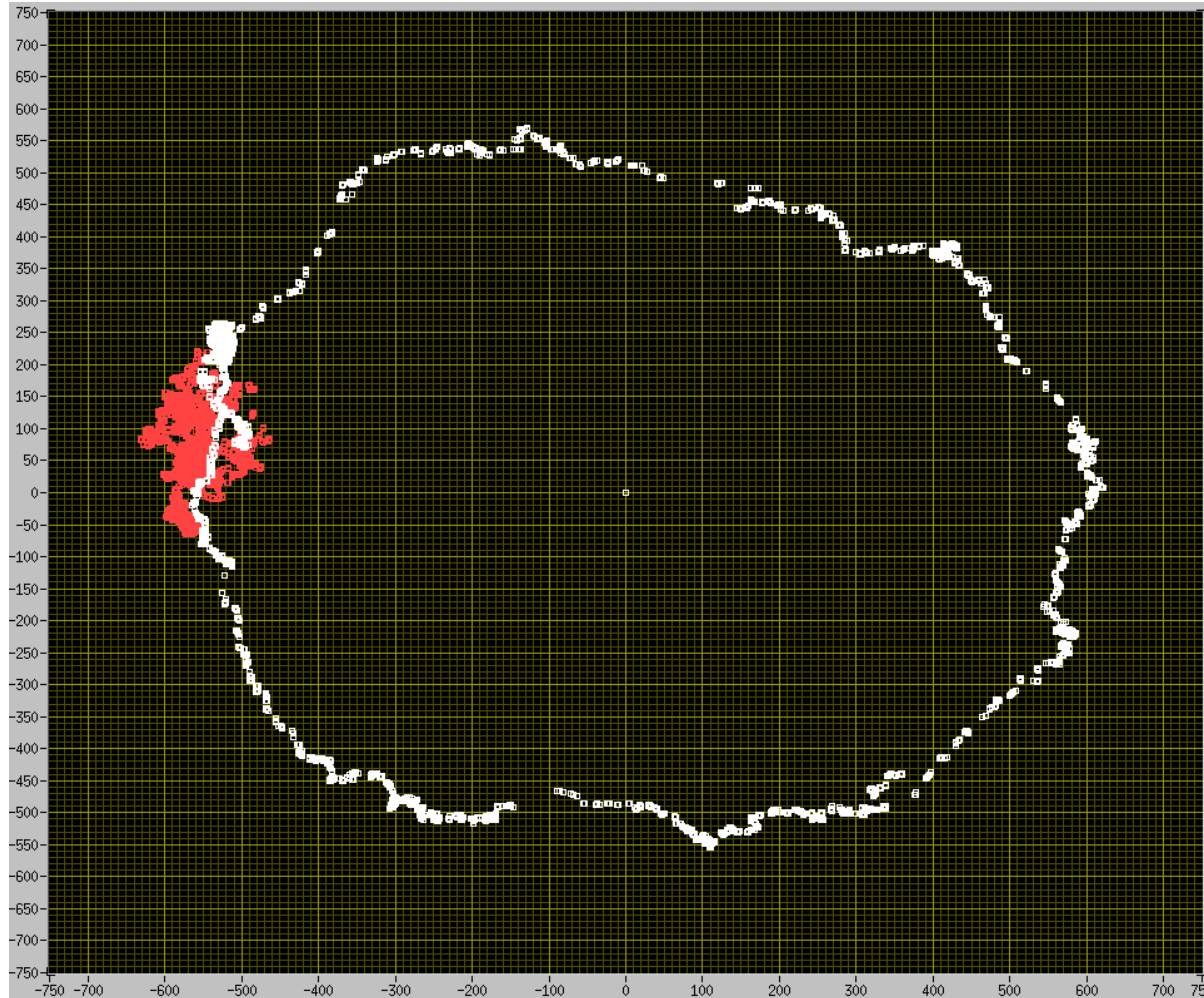


phase B: ω_2
phases A, C: ω_1

In order to obtain maximum S/N ratio for the MSB decision 'sector switching' is used. Dependent on rotor angle frequency ω_2 is switched to a different phase in order to obtain maximum signal amplitude, as shown above. This to stay in the yellow marked areas.

Note that even though the MCV delivers 2γ , this is enough information to determine which phase should use ω_2 for maximum output signal. So from a cold start at standstill the best phase for ω_2 can quickly be determined using just the MCV, without need for motor rotation.

Sector switching



Here $\dots e^{-j\xi}$ (white) and $\dots e^{-j(\xi-\gamma)}$ (red) are shown (full rotor rotation) with sector switching implemented. Note that the effective signal amplitude of $\dots e^{-j(\xi-\gamma)}$ with sector switching, for all rotor phases, is much larger than without sector switching. This results in a lower sigma Gaussian distribution curve for the MSB decision.

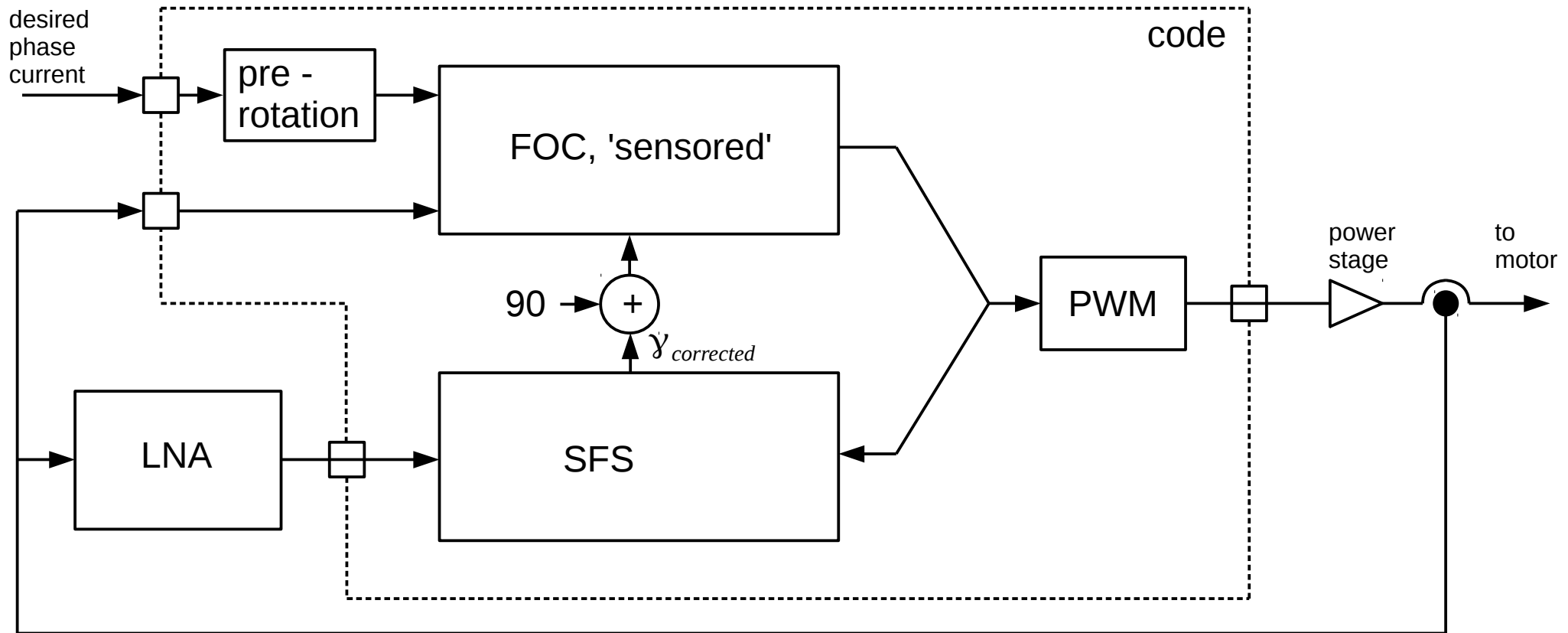
Use with FOC

The system described uses the high frequency PWM content to measure the phase of the total magnetic field. It can be used with a conventional 'sensored' FOC for motor control at standstill and low speed, from a cold start and without need for (initial) rotor movement.

- As γ indicates the angle of the total magnetic field as indicated by saliency (and not just the field of the rotor) the desired phase current presented to the FOC algorithm should be 'pre-rotated'. This to take into account the field from the phase current.
- The algorithm is motor speed limited:
 - The filters in the RX structures reduce the PQ signals at higher rotor speeds. Note that the PQ signals have double the frequency of the rotor speed !
 - The filters in the RX structures and the motors L/R cause a signal propagation delay. This can be compensated for using conventional techniques, but experiments have shown this to work only up to a delay of ~ 90 degrees.
 - The necessary filtering (and thus delay) depends on the analog S/N ratio, improving this with low noise high output current sensors, LNA and ADCs will increase speed.
- The algorithm is motor voltage limited:
 - The computation for the MCV as presented here limits the values for k, this limits the maximum PWM modulation and thus the maximum motor voltage. More Research will probably extend the usable voltage range of the SFS algorithm.
 - The B&D drill demo was limited to roughly 50% maximum output voltage.

With the B&D drill speeds in the range of 3 to 6 k-erpm were easily possible, more than enough for solid handover to sensorless FOC.

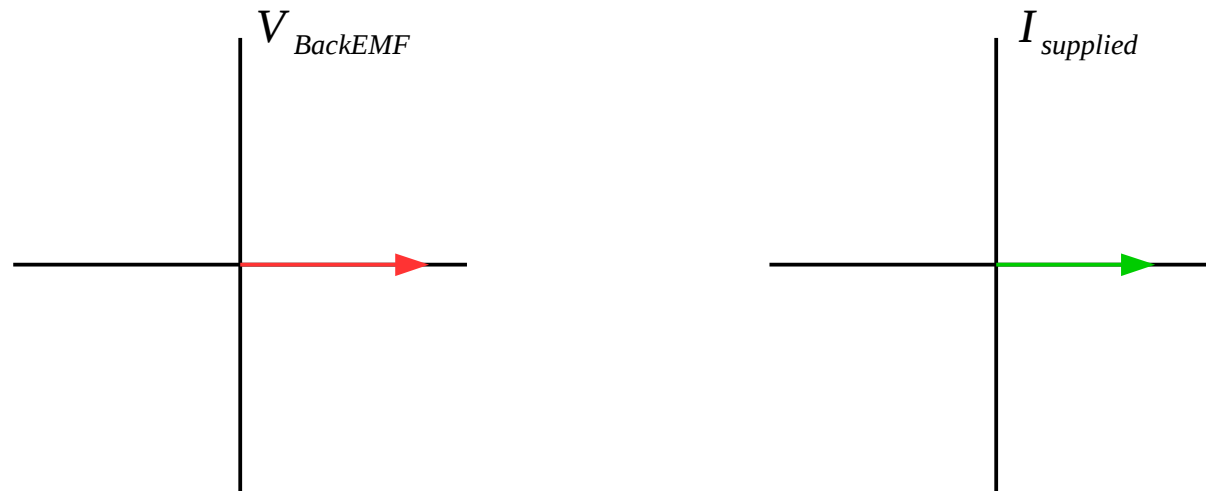
Use with FOC



The system described uses the high frequency PWM content to measure the phase of the total magnetic field. It can be used with a conventional 'sensored' FOC for motor control at standstill and low speed. For full speed applications, due to the filtering in the RX structure and the limitations on the maximum PWM modulation, at higher speed a handover to conventional sensorless FOC is necessary.

Verifying Saliency angle with Back EMF

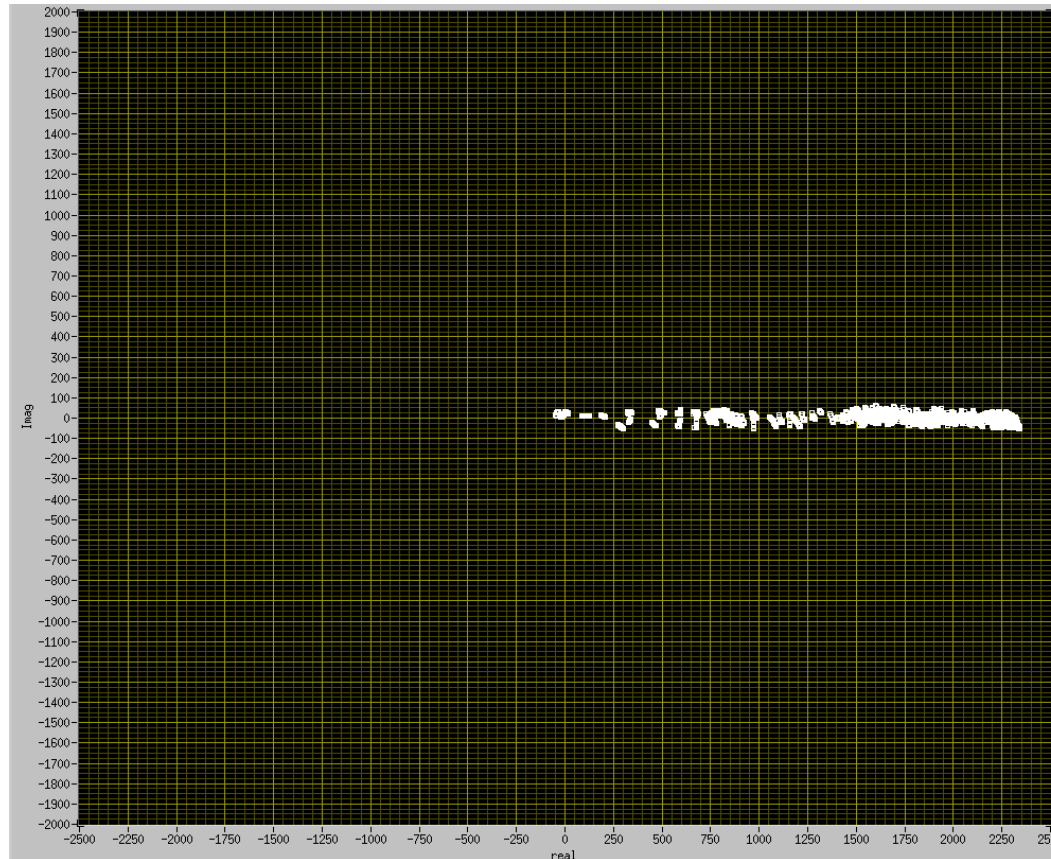
To get maximum output power (torque) for a given phase current the Back EMF (Bemf) voltage of the motor should be in phase with the supplied phase current. In my controllers the torque producing phase current is always on the real axis. For max torque the Back EMF voltage should therefore also be on the real axis:



With the SFS algorithm build into a FOC controller the relationship between saliency angle and Bemf voltage can be checked. For 0 A supplied phase current the controllers output voltage vector is equal to the motors Bemf voltage vector. So when the motor is spun up by hand the controllers output voltage should move along the real axis, providing the angle reported by the SFS algorithm is correct.

Verifying Saliency angle with Back EMF

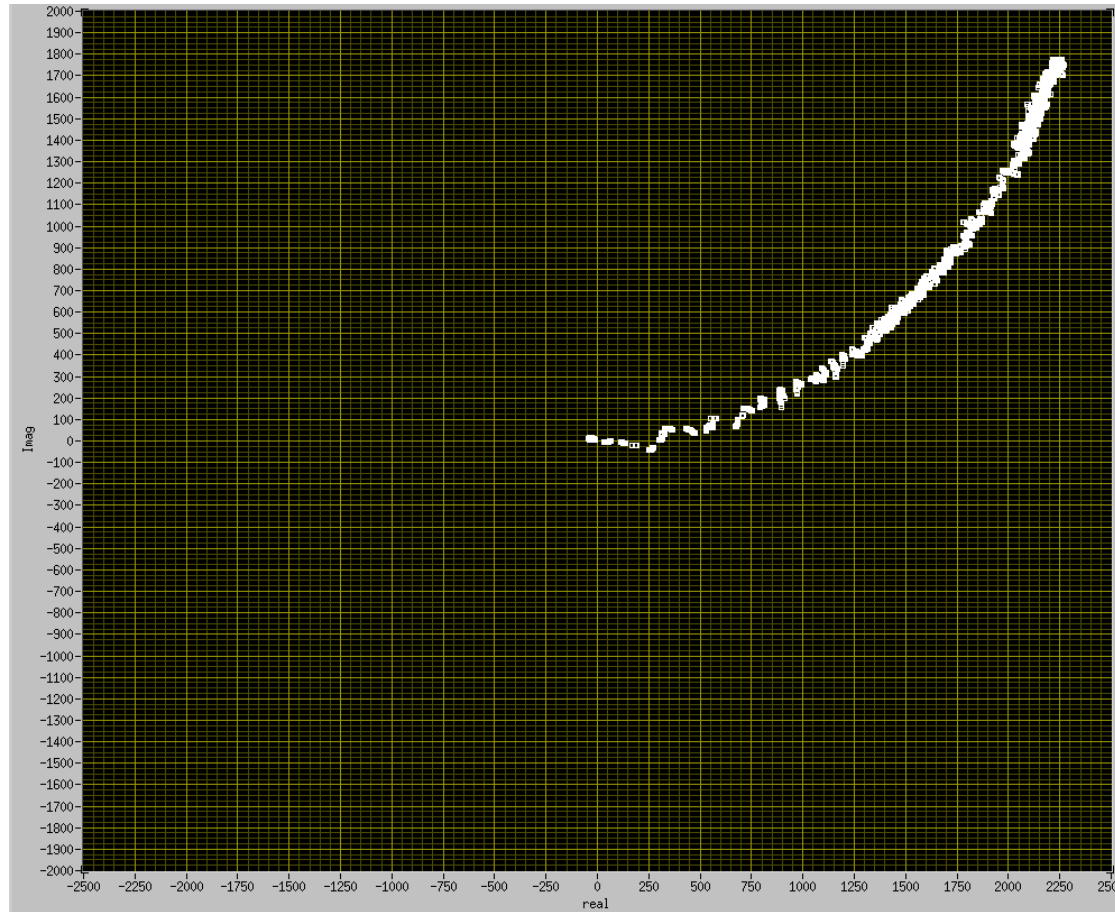
The picture below shows the reported voltage vector for increasing motor speed. The axis units are 1/32767th of the max output voltage.



The picture was made with correct delay compensation but without angle adjustment. None of my test motors needs angle adjustment, meaning that for all the Bemf voltage is in line with minimum inductance. I can imagine this is not the case for all motors. The test shown here can be used to check this and make adjustments if necessary.

Verifying Saliency angle with Back EMF

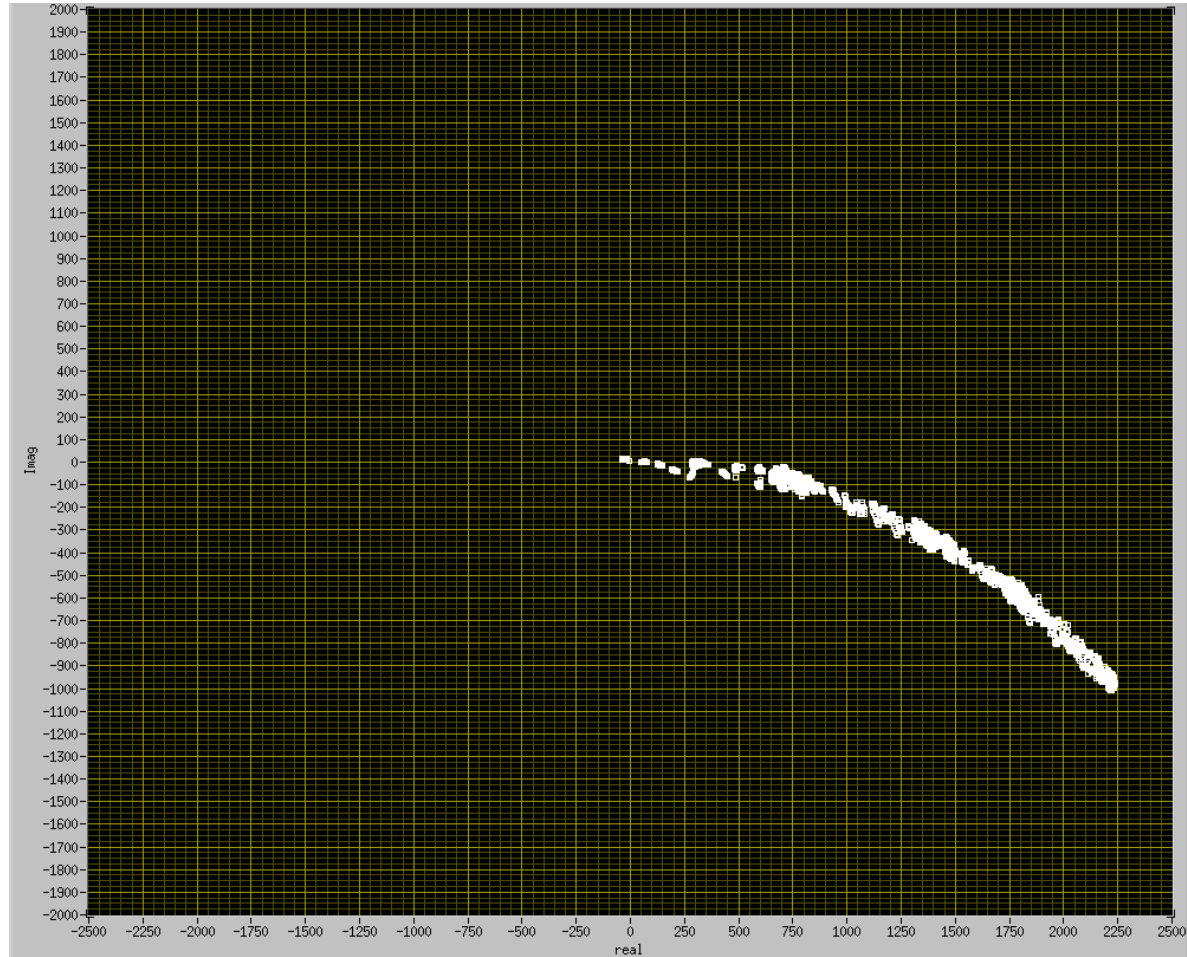
The picture below was made without compensating the delay in the filters of the receiver structures.



As speed goes up the voltage vector grows in length. Because the phase reported by the SFS algorithm is lagging, in order to match the motors B_{emf} the FOC controller must compensate by leading its voltage vector. For a filter with constant group delay the phase lag increases with motor speed.

Verifying Saliency angle with Back EMF

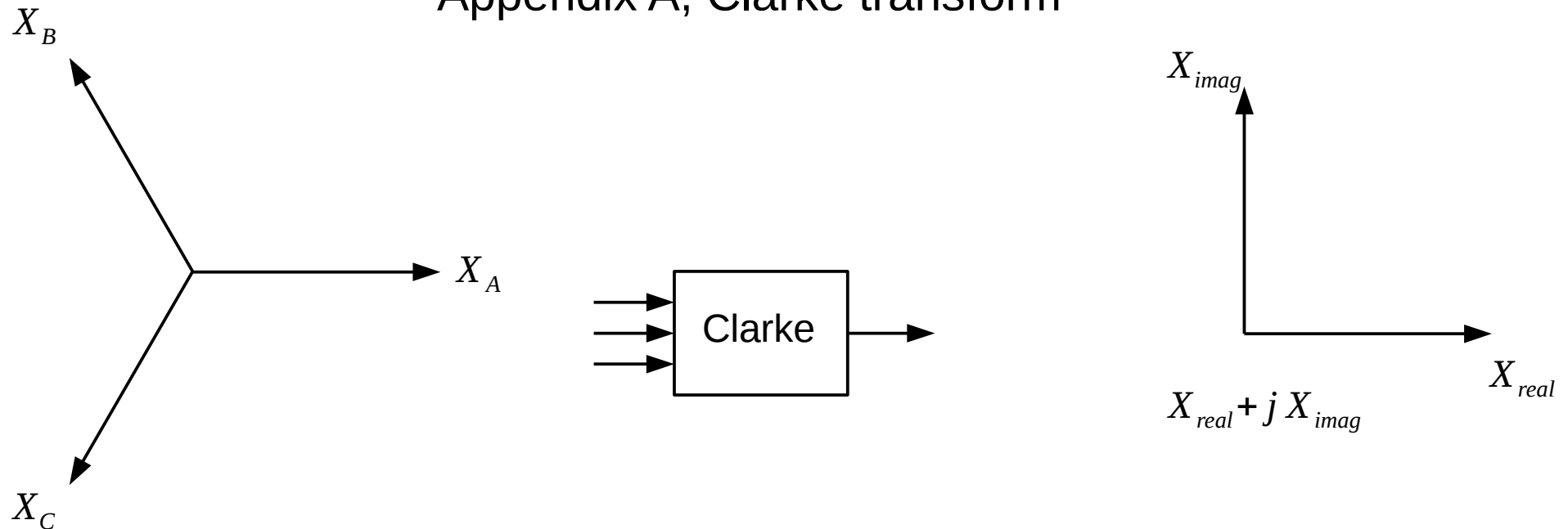
The picture below was made with more delay compensation than necessary.



Appendices

- A: Clarke Transform
- B: Receiver structure
- C: Making TX signals real
- D: Low side current sensing
- E: Frequency selection
- F: Hardware used and demo videos

Appendix A, Clarke transform



To project the 3 real valued 120 degree spaced amplitudes X_A , X_B and X_C onto a unit vector at angle α :

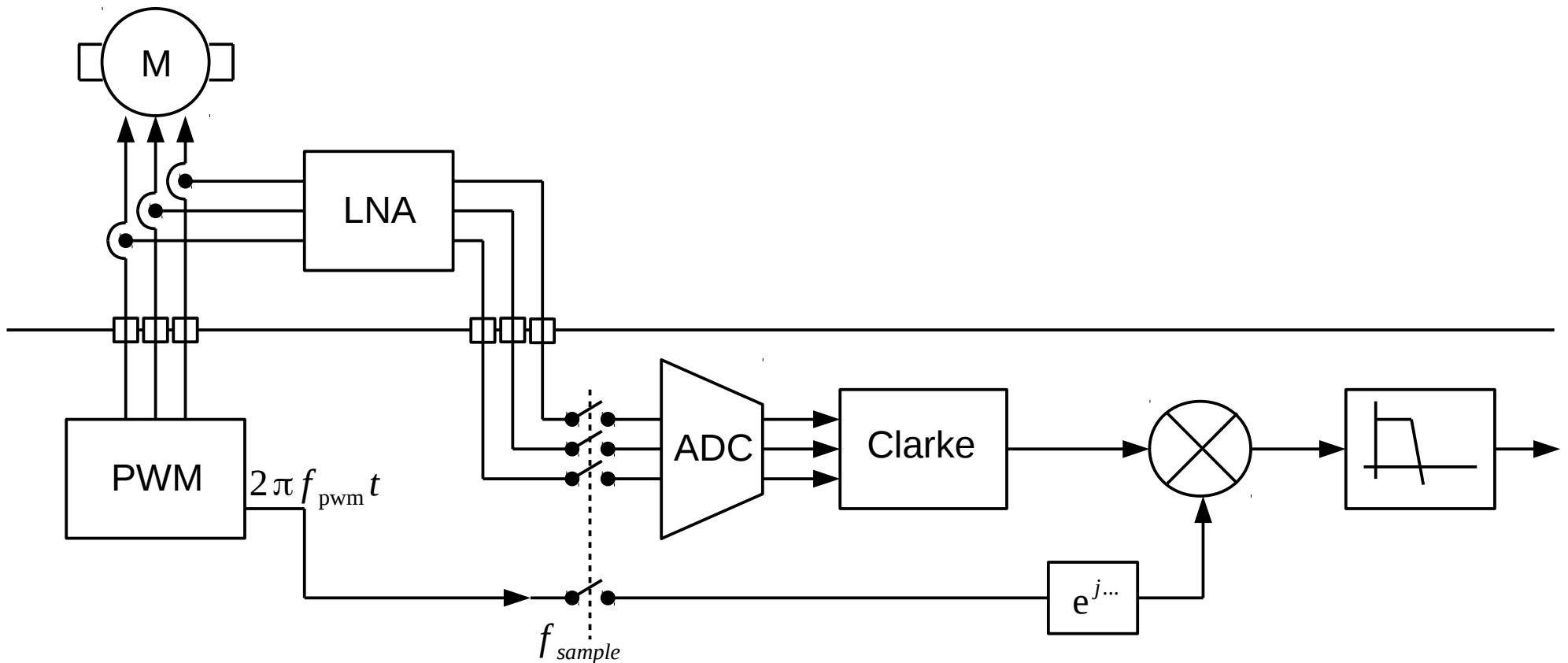
$$X_{real} + j X_{imag} = X_A e^{-j\alpha} + X_B e^{-j(\alpha + \frac{2}{3}\pi)} + X_C e^{-j(\alpha - \frac{2}{3}\pi)}$$

The Clarke transform is obtained when projecting onto the positive real axis, so for $\alpha=0$:

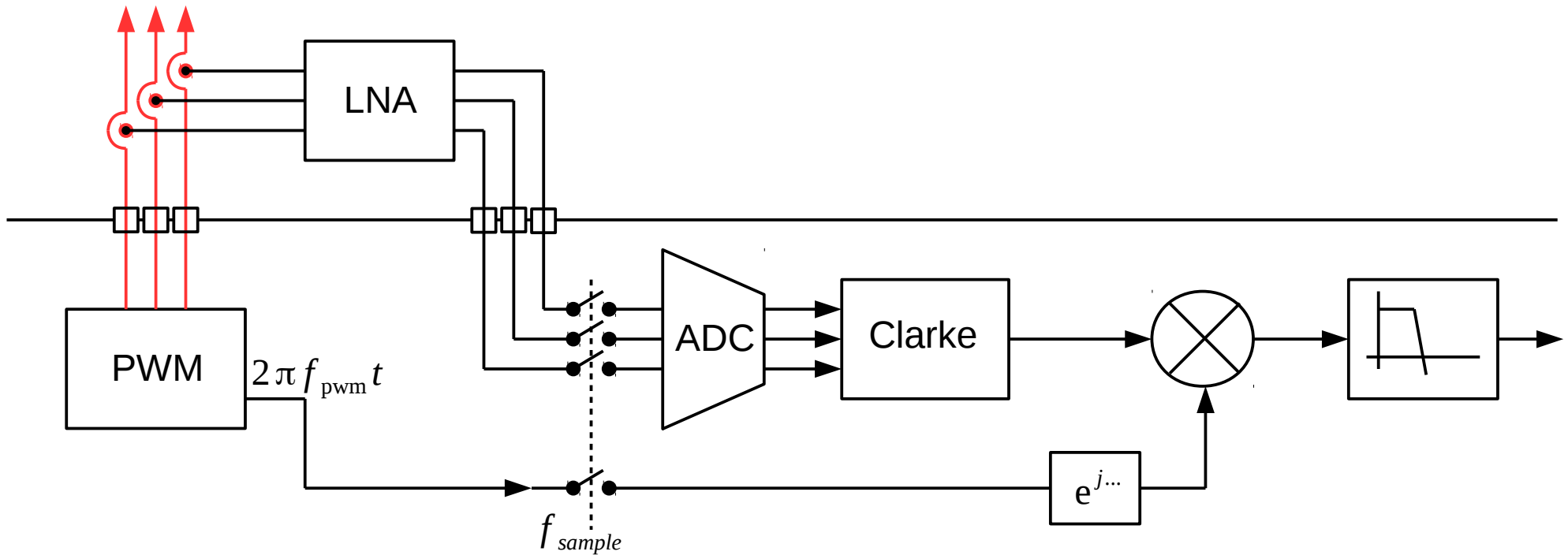
$$X_{real} + j X_{imag} = [X_A - \frac{X_B + X_C}{2}] + j \frac{1}{2} \sqrt{3} [X_C - X_B]$$

Appendix B, Receiver structure

A major part of the algorithm is finding the relative phase of the negative fundamental and the second harmonic. This is done using a Receiver structure, a classic direct conversion radio implemented in a combination of hard- and software.

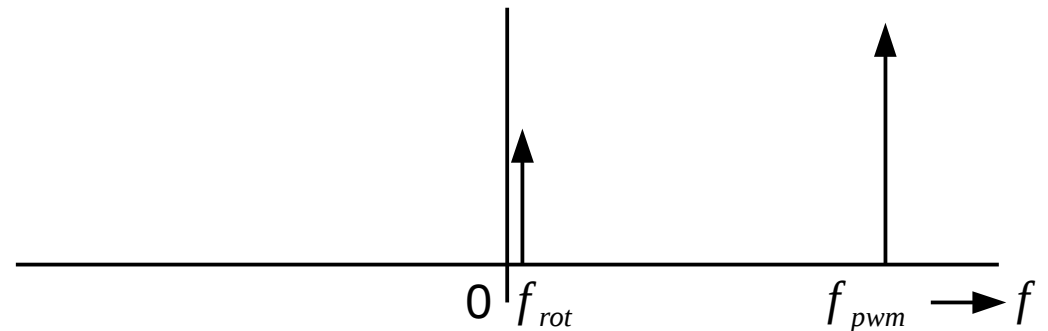


Appendix B, Receiver structure

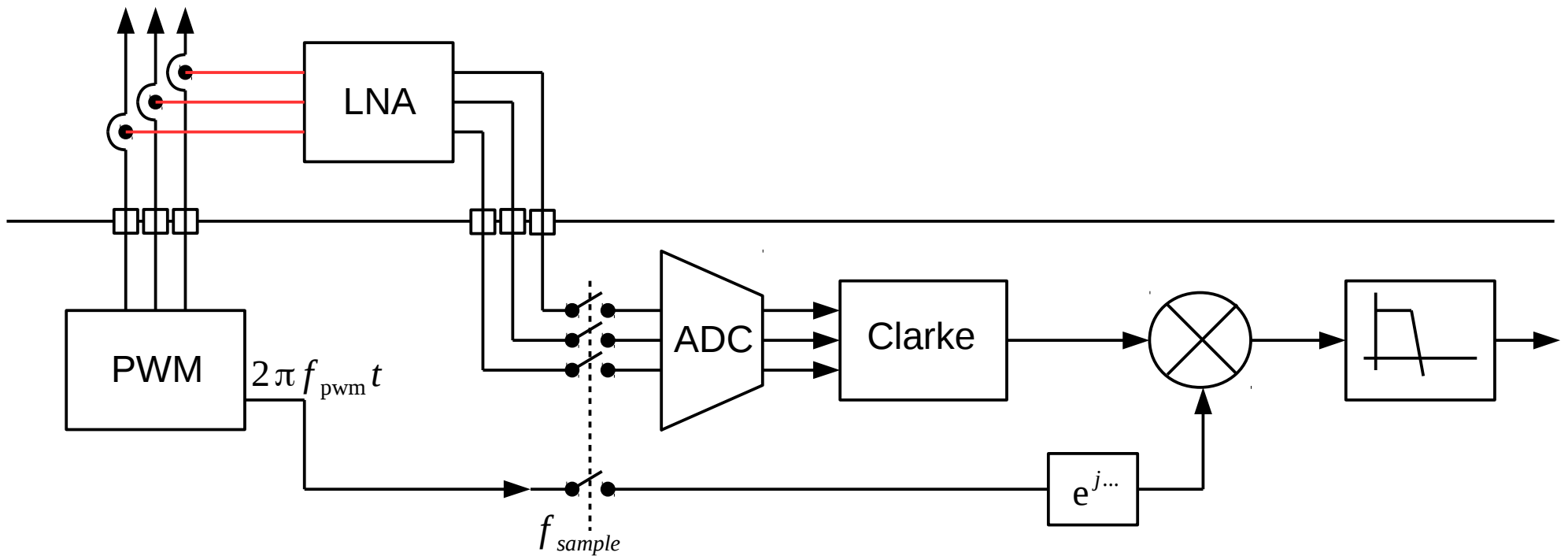


The following slides show how the receiver structure is used to find the phase of the negative fundamental. Only the relevant signals are considered.

The PWM signals to the motor contain two components, f_{rot} which makes the motor turn and the non-center aligned PWM frequency f_{pwm} .

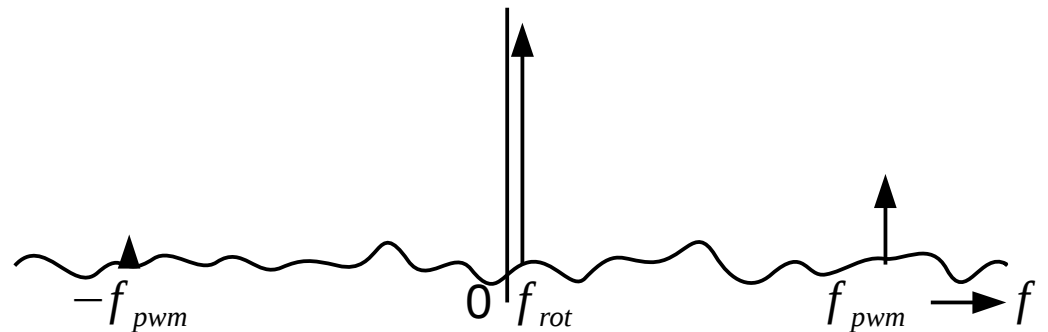


Appendix B, Receiver structure

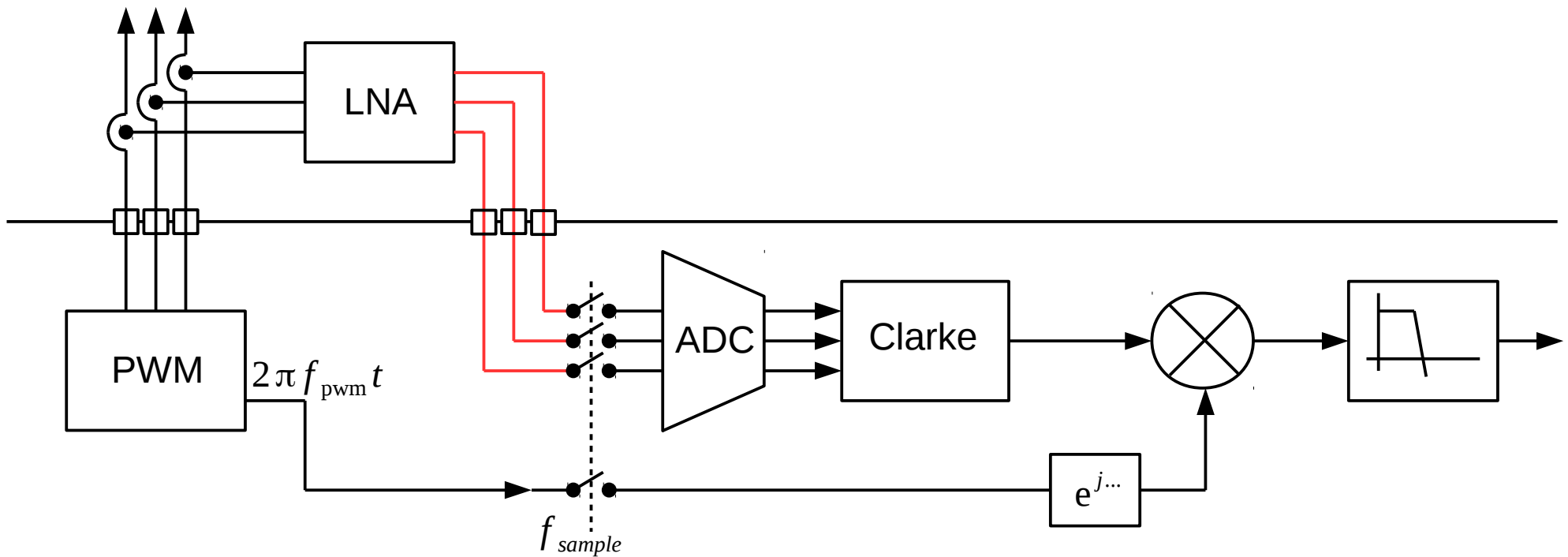


The motor currents, as picked up by the current sensors, contain the very strong motor rotating current f_{rot} and the PWM current at f_{pwm} .

As explained, motor saliency causes a small current at the negative PWM frequency $-f_{pwm}$. Also noise is picked up.

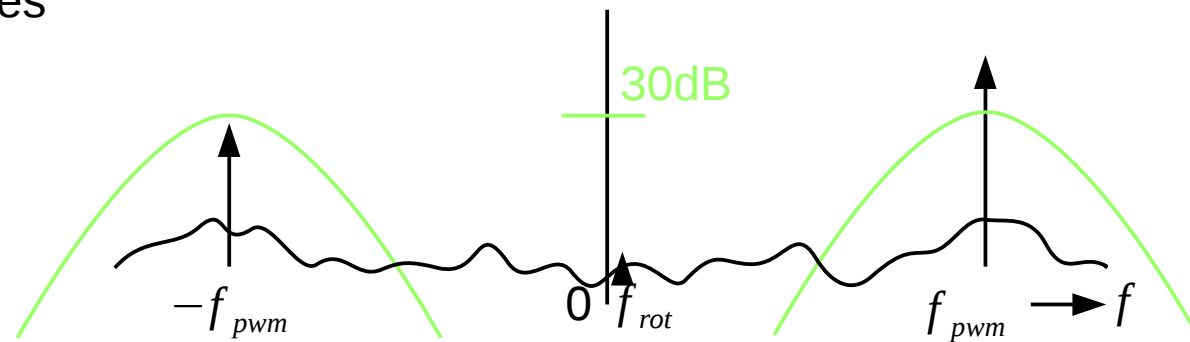


Appendix B, Receiver structure

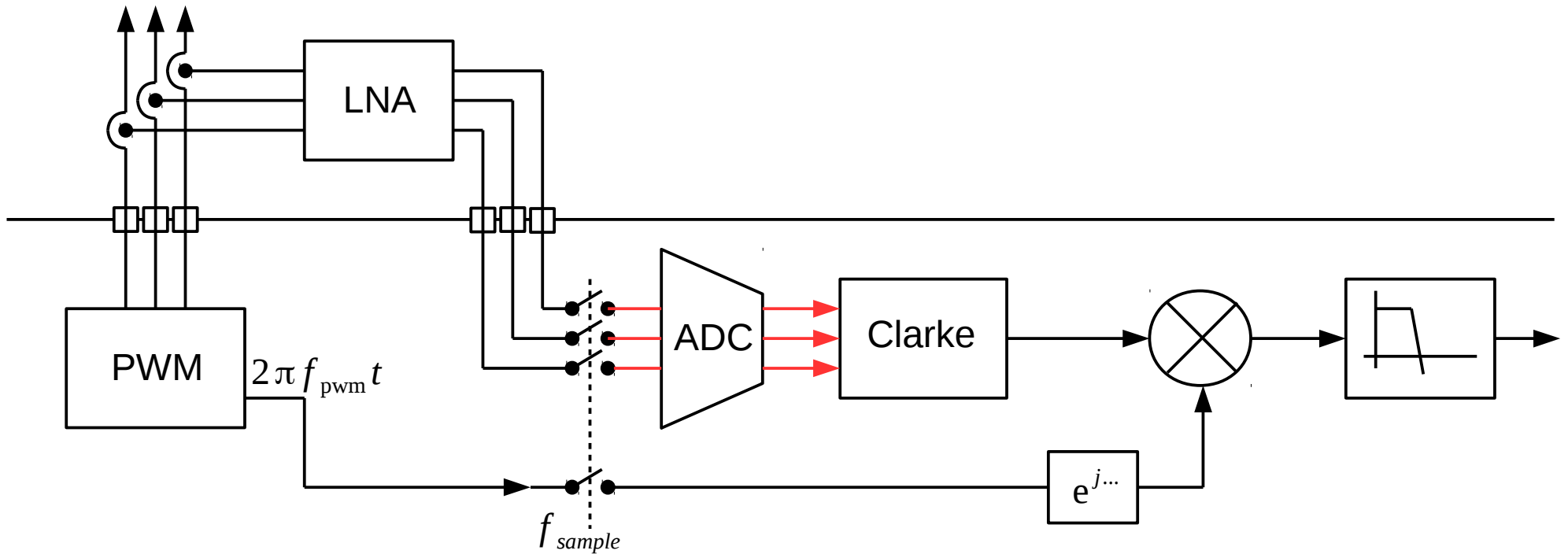


The Low Noise Amplifier (LNA) amplifies the relevant PWM frequencies and **strongly suppresses** f_{rot} . Its transfer function is highlighted in green.

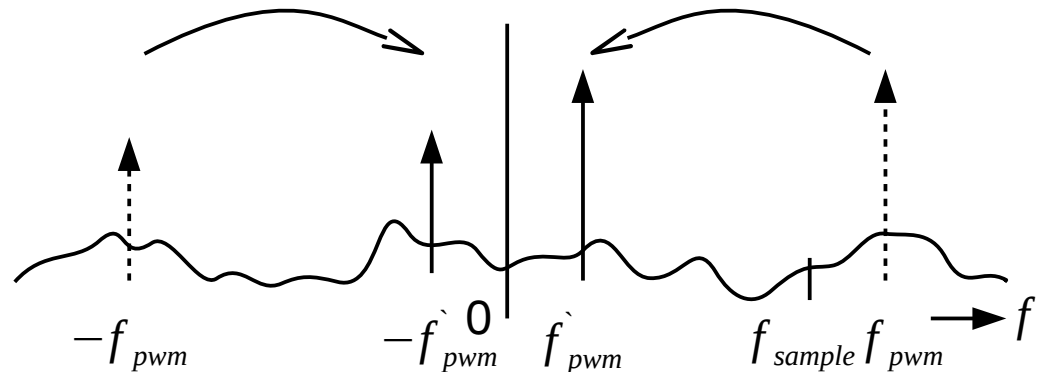
The LNA is built using conventional opamps, resistors and capacitors. Its gain is such that the maximum input range of the ADCs is used.



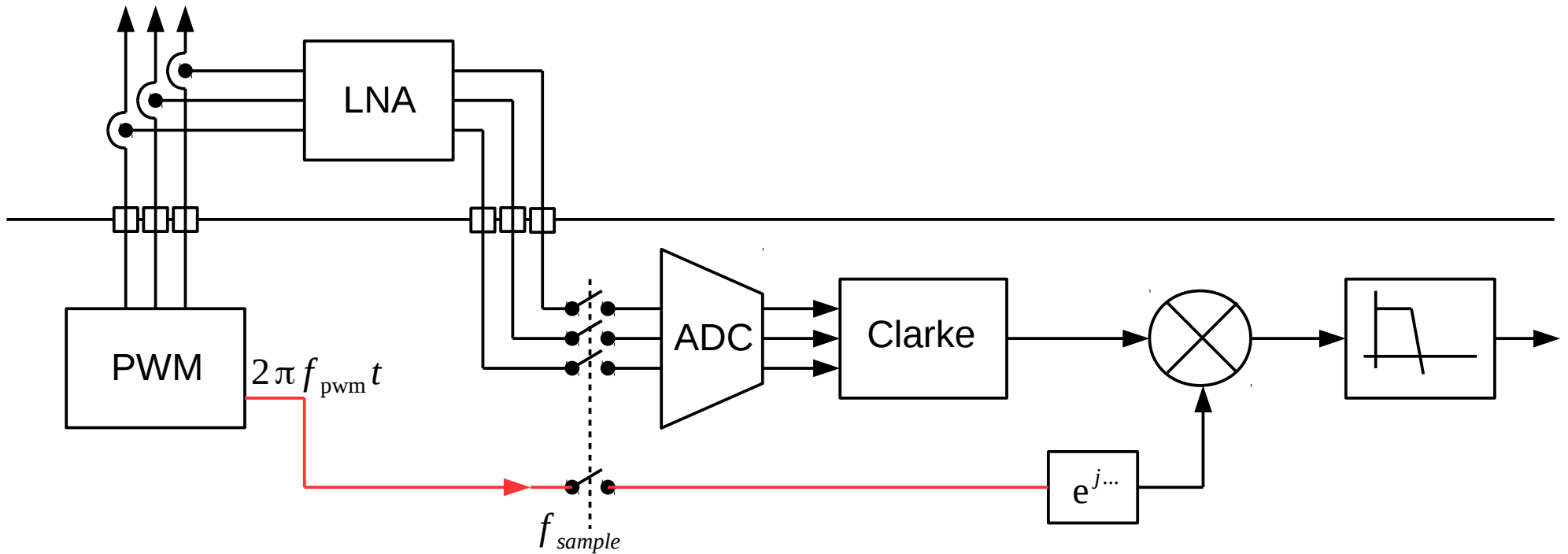
Appendix B, Receiver structure



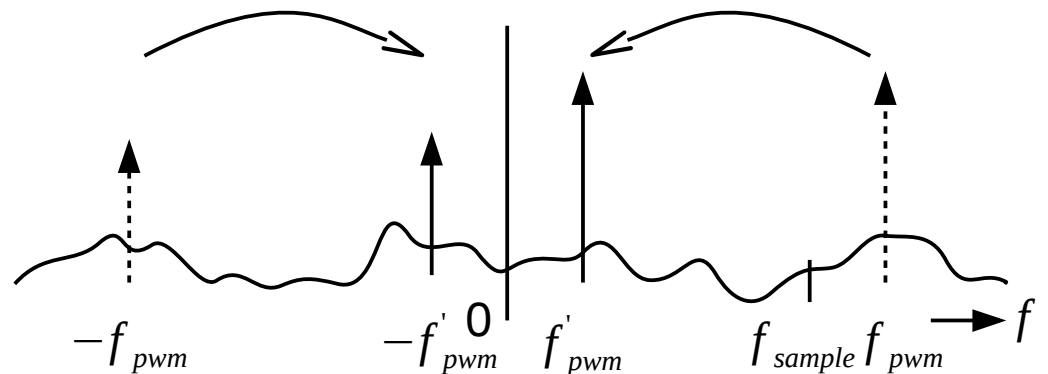
The algorithm runs on a frequency f_{sample} different from the PWM frequency. This causes aliasing / folding of all the signals. **Care must be taken that additional harmonics of the PWM signal do not obscure the wanted signal at $-f_{pwm}$.** (see Appendix E)



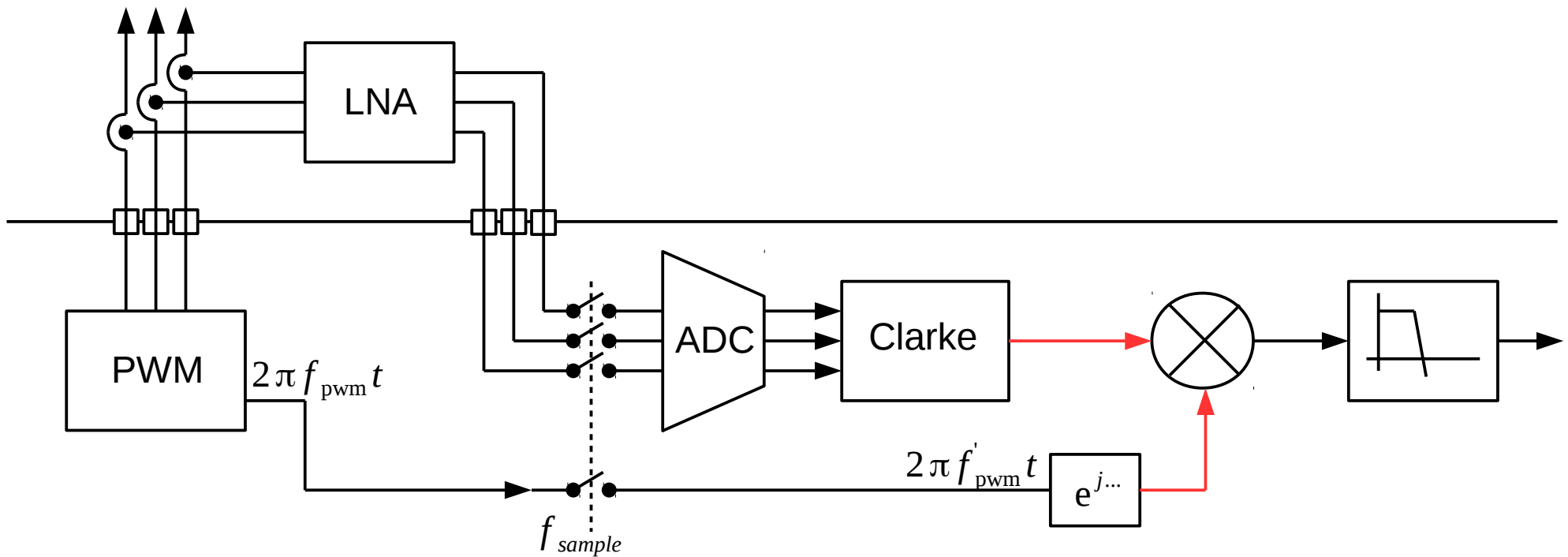
Appendix B, Receiver structure



The momentary phase ωt of the PWM signal is also sampled at f_{sample} . This causes it to correctly represent the phase of the new PWM frequency f'_{pwm} .

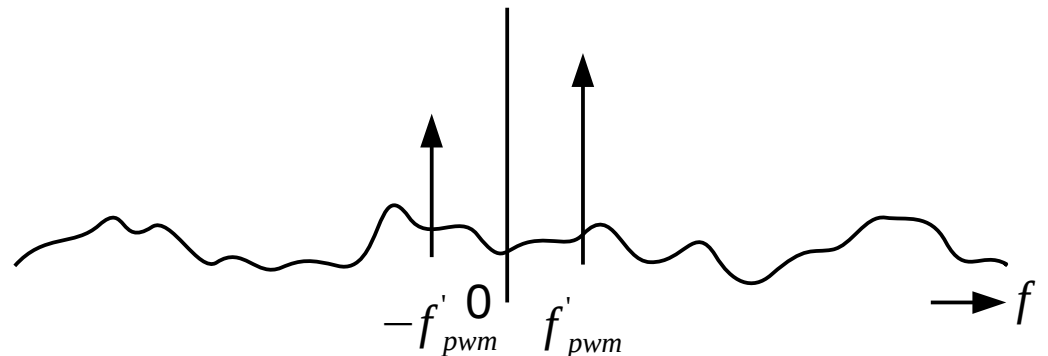


Appendix B, Receiver structure

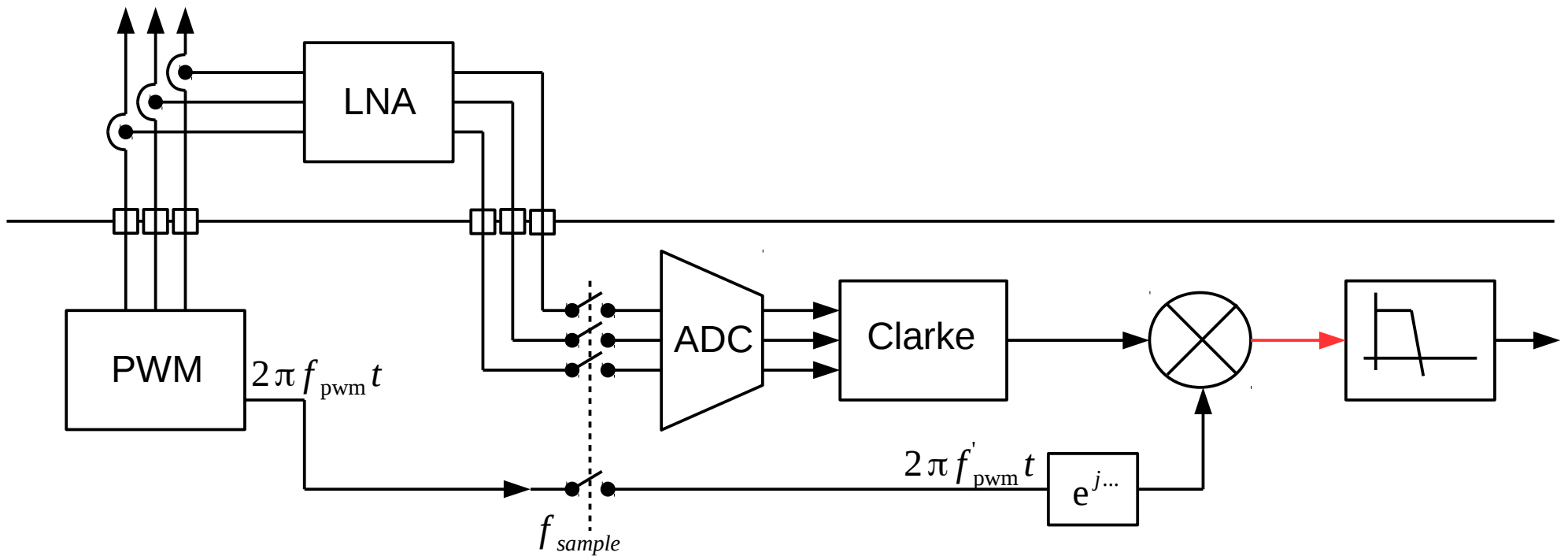


The complex signal out of the Clarke Transform block contains the wanted signal $I_e e^{j(2\gamma - 2\pi f'_{pwm} t)}$. Multiplication with $e^{j2\pi f'_{pwm} t}$ shifts the entire spectrum by f'_{pwm} .

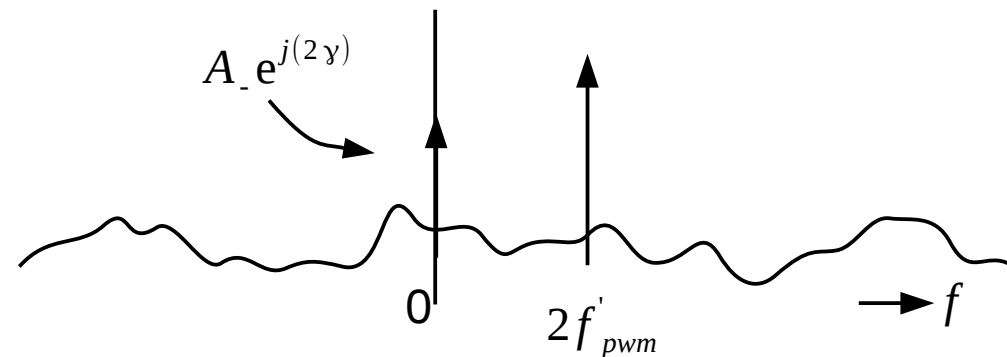
Note that $2\pi f'_{pwm} t$ is a phase, and that $e^{j\dots}$ can be implemented with a sine / cosine lookup table.



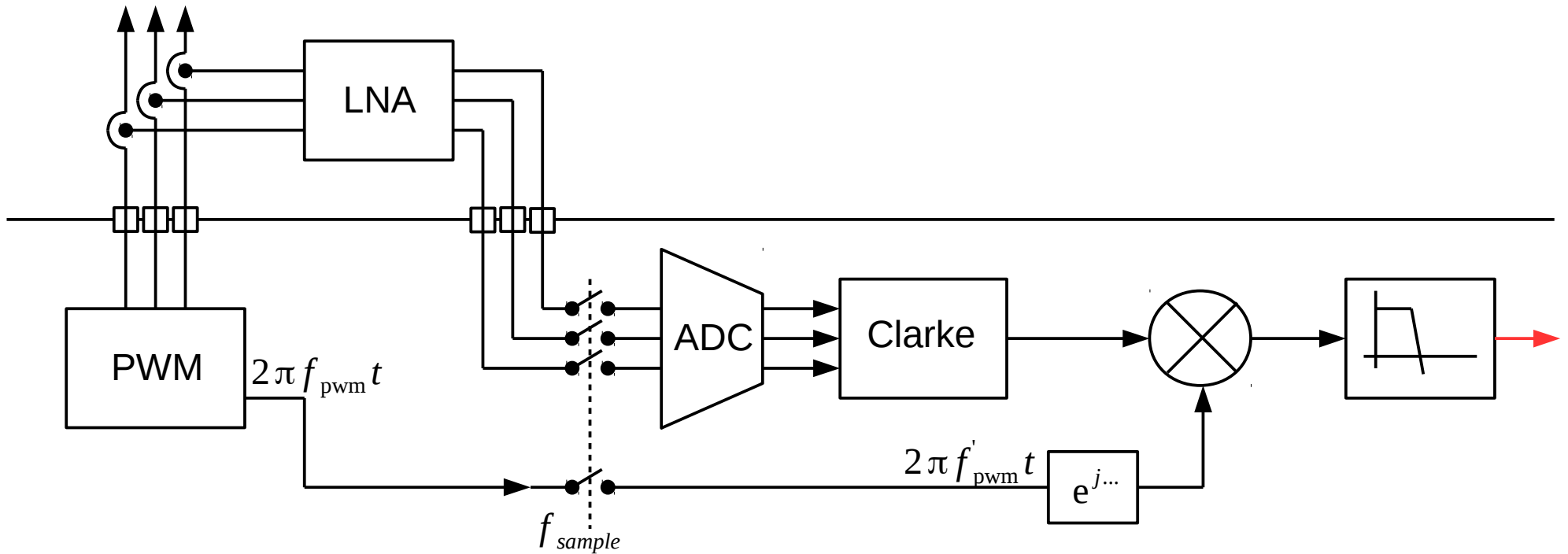
Appendix B, Receiver structure



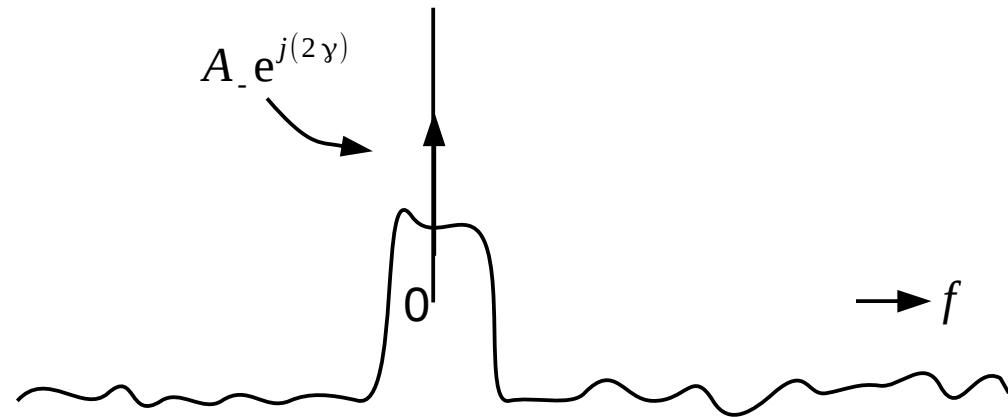
The component at 0 Hz now contains the wanted phase information γ . The signal further contains a certain amount of noise and unwanted frequency components which have to be removed using a digital filter



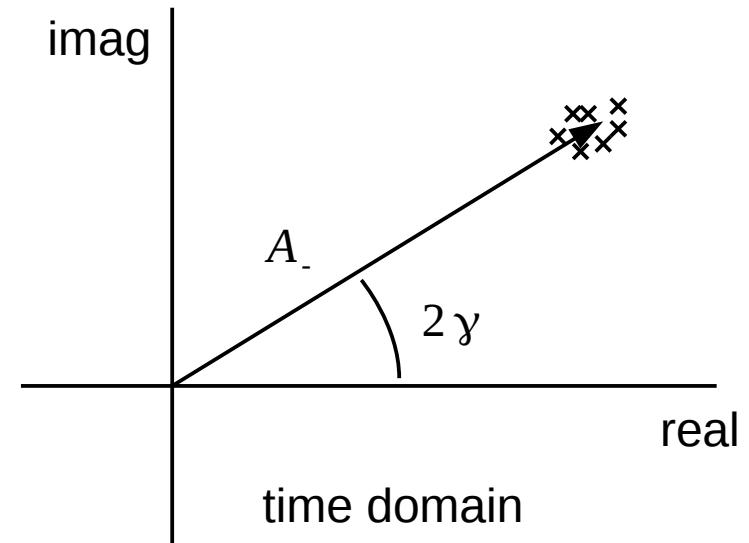
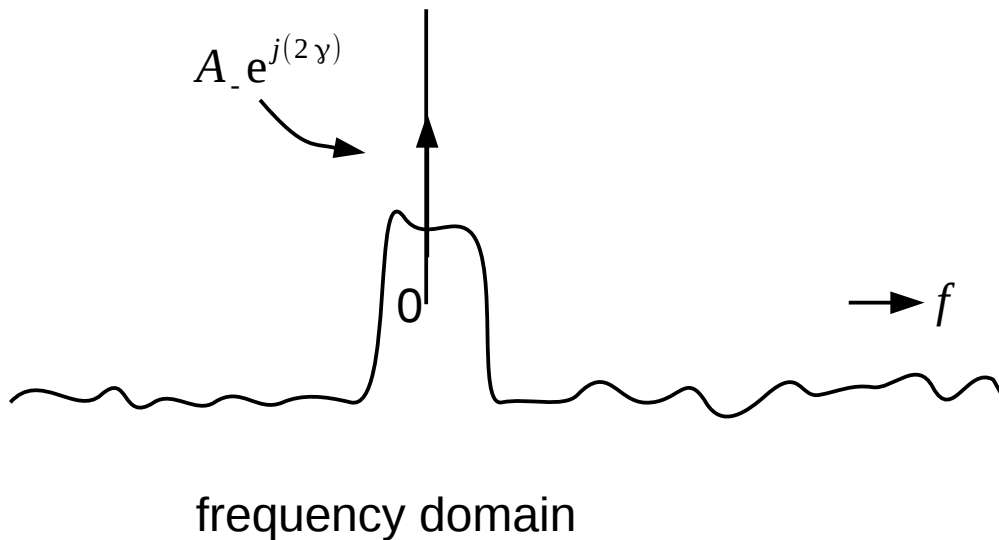
Appendix B, Receiver structure



The final digital filter has a very narrow bandwidth to remove as much noise as possible, but should be wide enough to allow the phase 2γ to have a certain increase with time (when the motor is running 2γ increases linear with time, it becomes $4\pi f_{motor_speed} t$ with f_{motor_speed} the frequency the motor is running at)



Appendix B, Receiver structure



The component $A_e^{j(2\gamma)}$ at double the rotor speed in the frequency domain corresponds to a constant stream (one every f_{sample}) of complex numbered samples in the time domain. The remaining noise means the subsequent complex numbers are not a single point but form a cloud in the complex plane. The larger the noise, the larger the area of the point cloud.

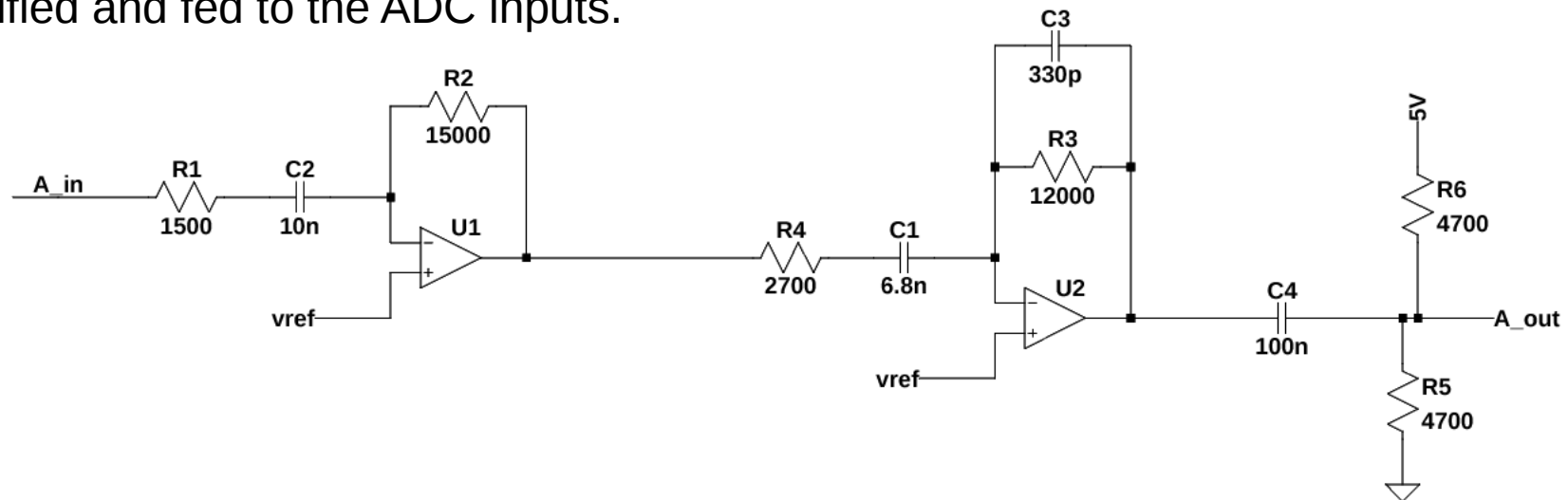
A CORDIC or arctan function can be used to extract the phase information 2γ from a complex number.

Appendix B, Receiver structure



There are several options for the LNA, dependent on how many ADC channels are available:

- Two ADC channels. With two current sensors the current sensor outputs can be filtered, amplified and fed to the ADC inputs.

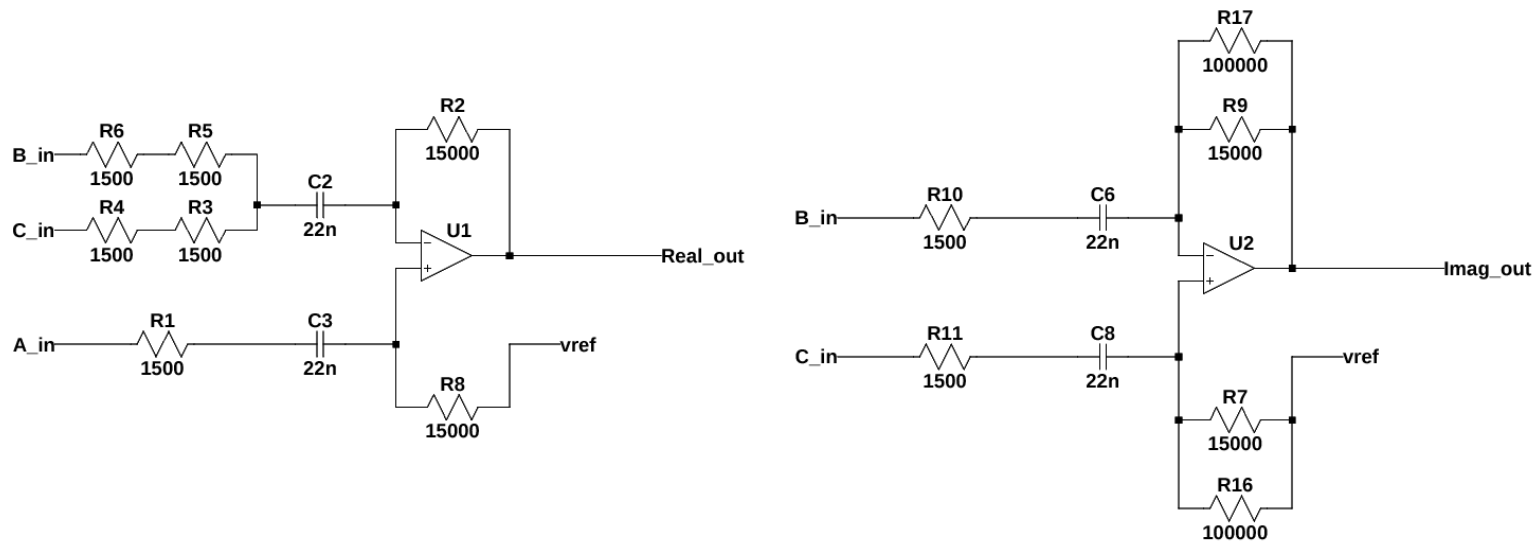


The filter transfer is chosen such that the signals of interest are amplified to the full input range of the ADC's, while removing as much as possible the low frequency motor currents. Here two opamps per path are shown, dependent on required gain and filtering one opamp per path should be enough.

Appendix B, Receiver structure



Another option for two ADC channels is to move the Clarke transform into the analog domain.



The picture above replaces the first opamp of the previous slide, filtering of Real_out and Imag_out can continue with R4 / U2 of the previous slide.

The analog Clarke transform can be adapted for two current sensors.

Appendix B, Receiver structure



- Three ADC channels. With three current sensors the current sensor outputs can be filtered, amplified and fed to the ADC inputs. This option uses independent filters for each channel.
- Four ADC channels. With this option two different filters are implemented, a real filter for the main PWM tone and a second complex filter for the sum / difference of the two PWM tones.
The filtering process starts with the analog Clarke transform. For the main PWM tone the real and imag signal are further (independent) amplified and filtered, requiring two ADC channels.
For the sum / difference of the two PWM tones an asymmetric complex filter amplifying only the single signal of interest makes sense. This is possible using the real and imag signal coming from the Clarke transform. As more noise and unwanted signals are suppressed, more amplification can be provided for the frequency of interest.

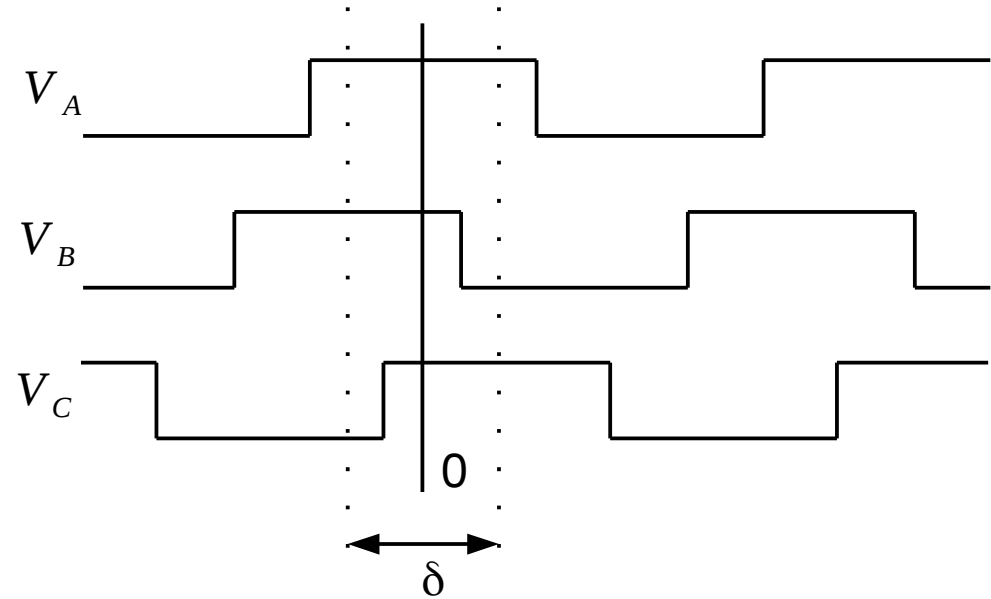
Appendix C, making TX signals real

To recap, the TX signals must be kept real for the simple MCV equation to be correct. As the motor powering signals get larger the amplitude of the fundamentals in the PWM signals change and measures must be taken.

$$V_A = A_A \cos(\omega t) = \frac{A_A}{2} [e^{j\omega t} + e^{-j\omega t}]$$

$$V_B = A_B \cos(\omega t + \frac{\delta}{2}) = \frac{A_B}{2} [e^{j(\omega t + \frac{\delta}{2})} + e^{-j(\omega t + \frac{\delta}{2})}]$$

$$V_C = A_C \cos(\omega t - \frac{\delta}{2}) = \frac{A_C}{2} [e^{j(\omega t - \frac{\delta}{2})} + e^{-j(\omega t - \frac{\delta}{2})}]$$



Applying the Clarke transform:

$$V_{real} + jV_{imag} = e^{j\omega t} \left[\frac{A_A}{2} + \frac{A_B}{2} e^{j(\frac{\delta}{2} - 2\pi/3)} + \frac{A_C}{2} e^{-j(\frac{\delta}{2} - 2\pi/3)} \right] + e^{-j\omega t} \left[\frac{A_A}{2} + \frac{A_B}{2} e^{j(\frac{\delta}{2} + 2\pi/3)} + \frac{A_C}{2} e^{-j(\frac{\delta}{2} + 2\pi/3)} \right]$$

Appendix C, making TX signals real

With the phase difference between V_B and V_C fixed, the two remaining degrees of freedom are a common phase shift for V_B and V_C , and a phase shift for V_A . The important thing is to keep the TX signals real (see the derivation of the equation for the MCV), their amplitudes may change. The algorithm for TX signal correction runs for every cycle of the PWM output, as every cycle the PWM signals must be corrected based on their momentary duty cycle. The following steps are taken:

- With the duty cycles known, calculate the amplitudes of the fundamental, A_A , A_B and A_C using

$$A_x = \frac{2V}{\pi} \sin(\pi DC_x)$$

- Calculate the (complex) contributions to the TX signals coming from A_B and A_C .
- Rotate so obtained positive and negative TX signals such that their imaginary parts are equal in size but of opposite polarity. This gives the common phase shift for V_B and V_C .
- Calculate the rotation of A_A such that its imaginary contributions to the positive and negative TX signals cancel those of A_B and A_C . This gives the phase shift for V_A .
- Important: as the amplitudes of the positive and negative TX signals will have changed, a new value for k must be calculated for use in the MCV computation !

Appendix D, low side current sensing

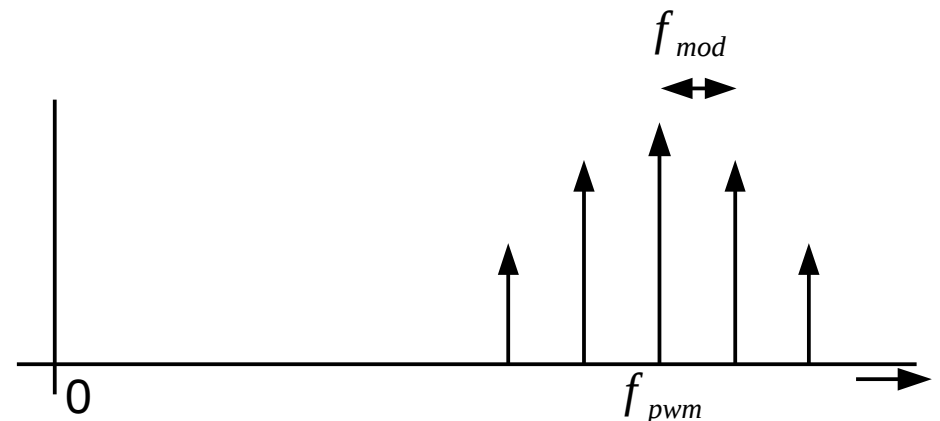
The method as outlined so far assumes current sensors in the motor wires. For a low cost solution current sensing in the low side NMOS sources is more desirable.

The method is based on being able to measure the spectral components of the PWM signal. To this order the sample frequency at which the algorithm runs is different from the PWM frequency.

The classic low side current sensing algorithm work with the sampling frequency of the algorithm being the same as the PWM frequency. In this case the PWM frequency components, after sampling, are indistinguishable from DC.

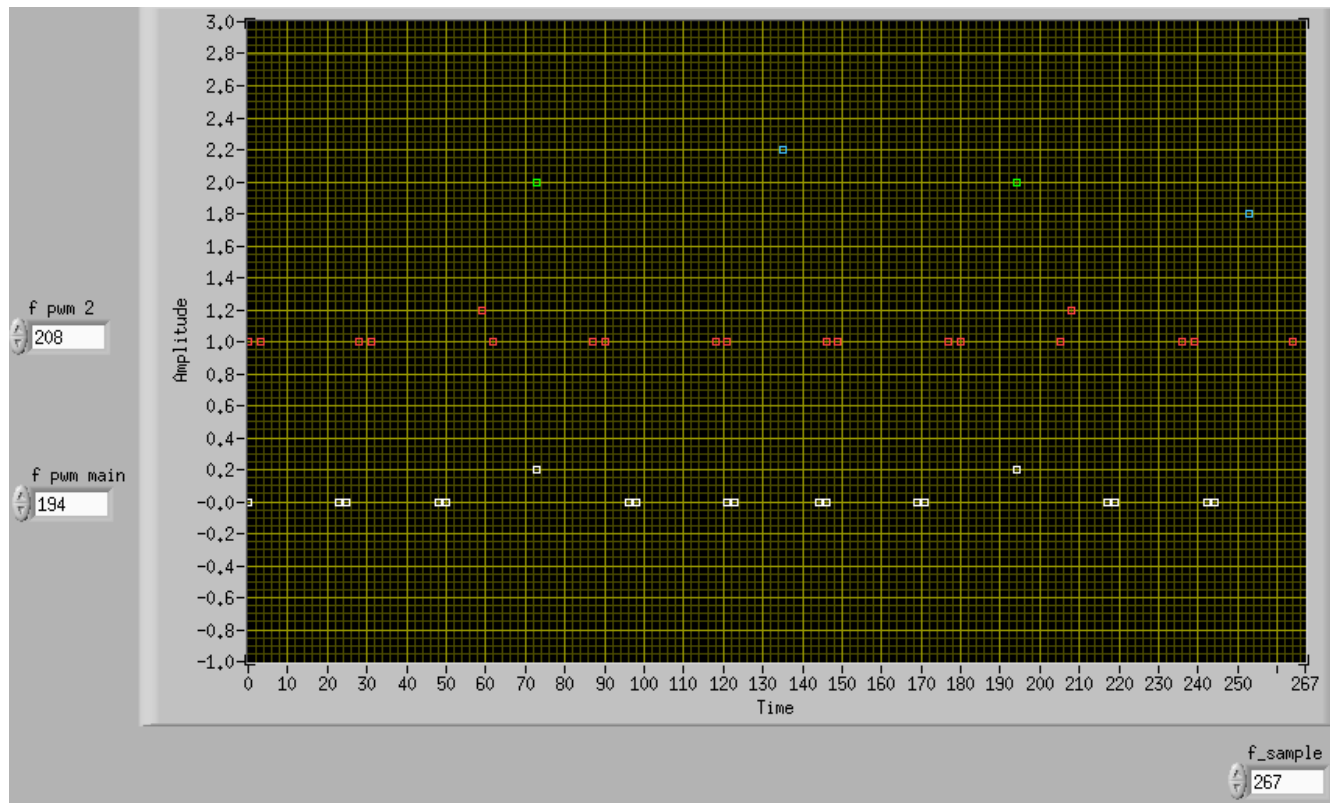
One option might be to generate high frequency signals for saliency detection is to phase-modulate the PWM frequency. Phase modulation (PM) can generate the high frequency tones necessary for saliency detection while still enabling current sampling at the PWM frequency.

$$x(t) = A \sin(\omega_{pwm} t + \phi_{mod} \sin(2\pi f_{mod} t))$$



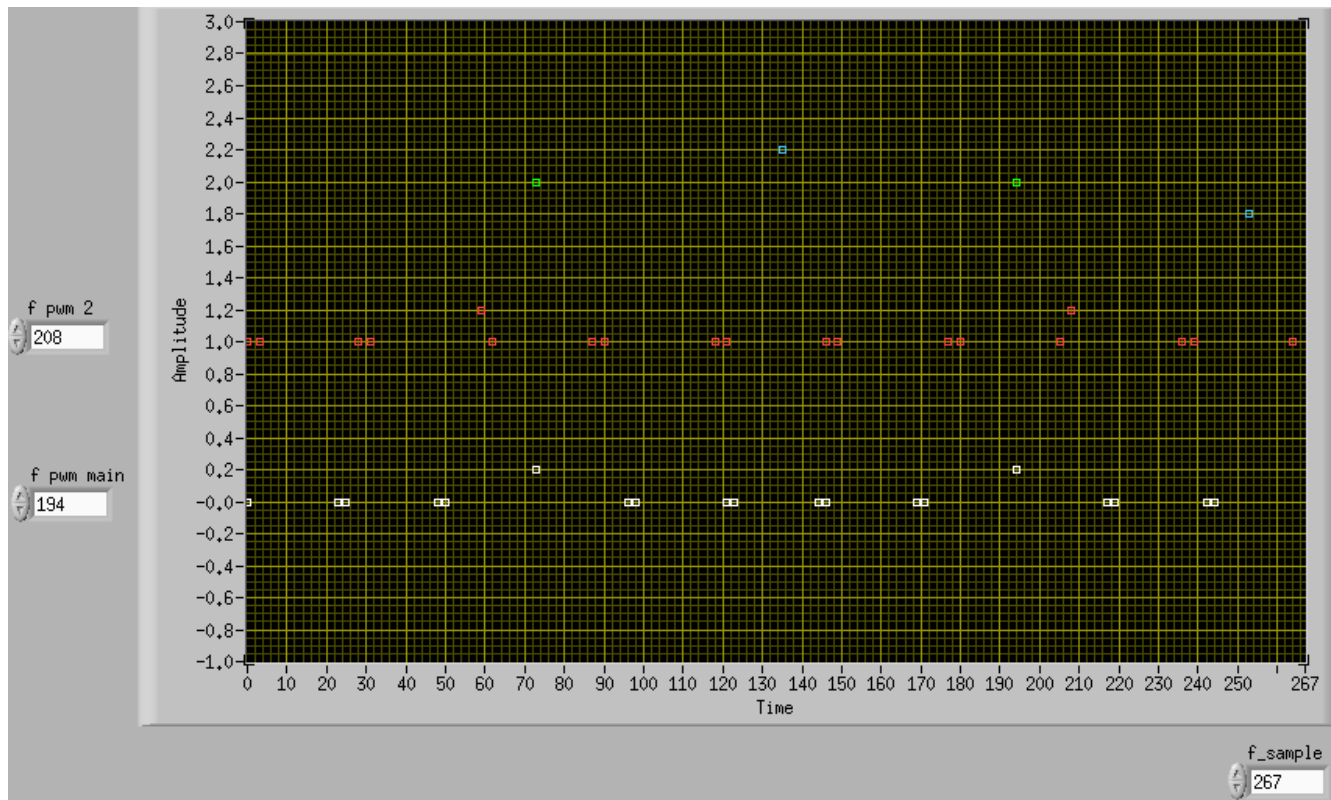
Appendix E, frequency selection

The choice of ADC sampling frequency and PWM frequencies is very important for the correct operation of the SFS algorithm. The square wave TX signals as outputted by the controller contain many harmonics of unknown amplitude. These harmonics, after sampling and aliasing, should not obscure the frequencies of interest.



The figure above is the output of a program used to select the ADC sampling frequency f_{sample} (x-axis) and the two PWM frequencies $f_{\text{pwm_main}}$ and f_{pwm_2} .

Appendix E, frequency selection



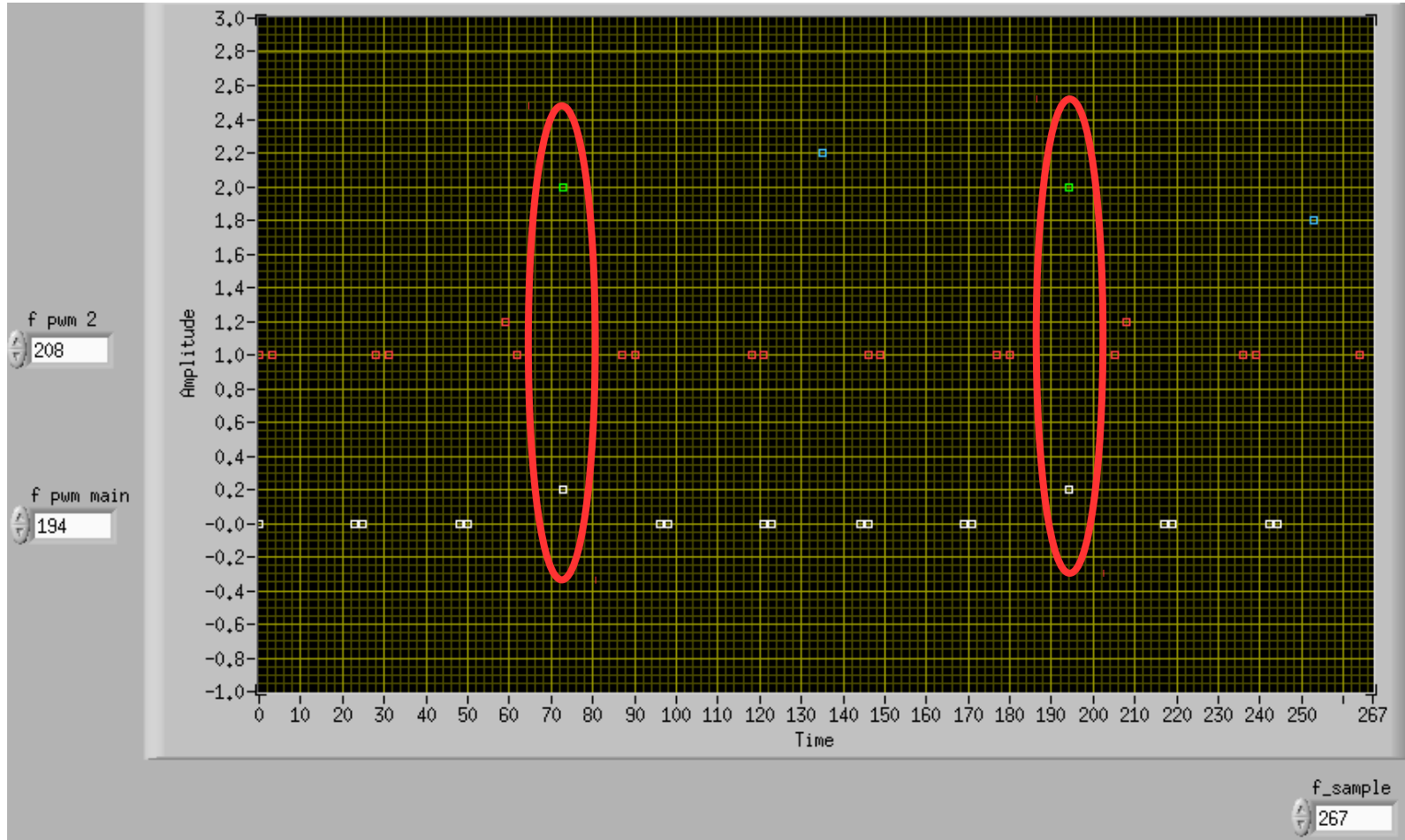
The frequencies are in units of 100Hz, so the sampling frequency in the picture is 26.7 kHz.

The tool shows the location (after aliasing) of the first 9 positive and negative harmonics for the main and second PWM frequency.

The white dots on the 0.0 (y-axis) line show the location of the harmonics of the main PWM frequency, with the fundamentals at the 0.2 line. The second PWM frequency and its harmonics are shown in red on the 1.0 and 1.2 line.

The green dots on the 2.0 line are the fundamentals of the main PWM frequency and represent the location of the PQ signals. The blue dots represent the sum (at 2.2) and difference (at 1.8) frequencies, used for deciding the 0 / 180 degrees as discussed.

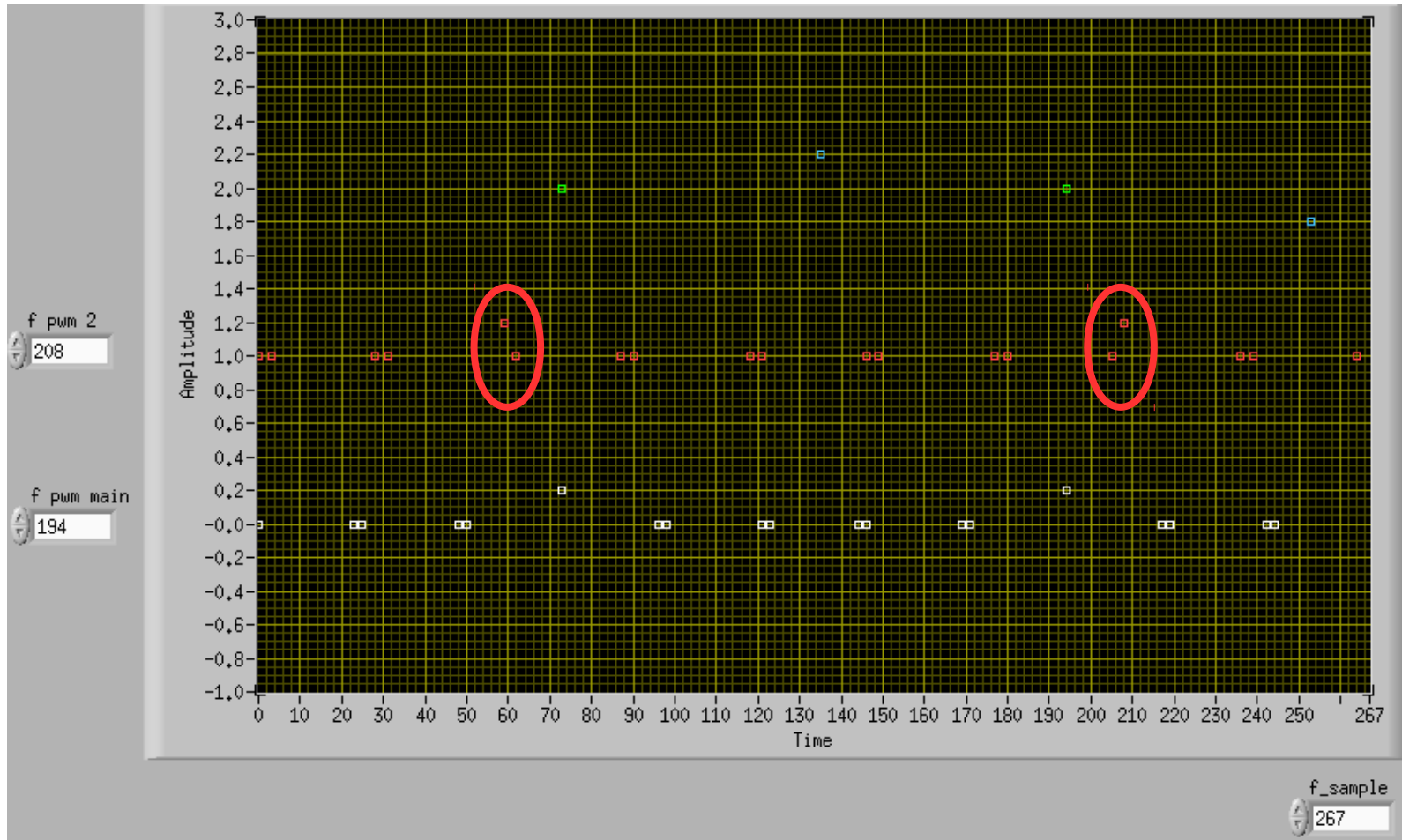
Appendix E, frequency selection



For clean PQ signals the main PWM frequency should have lots of empty spectrum around it. Both positive and negative fundamentals are important. The main PWM frequency must not be obscured by the second PWM frequency (for the 0/180 deciding part of the algorithm).

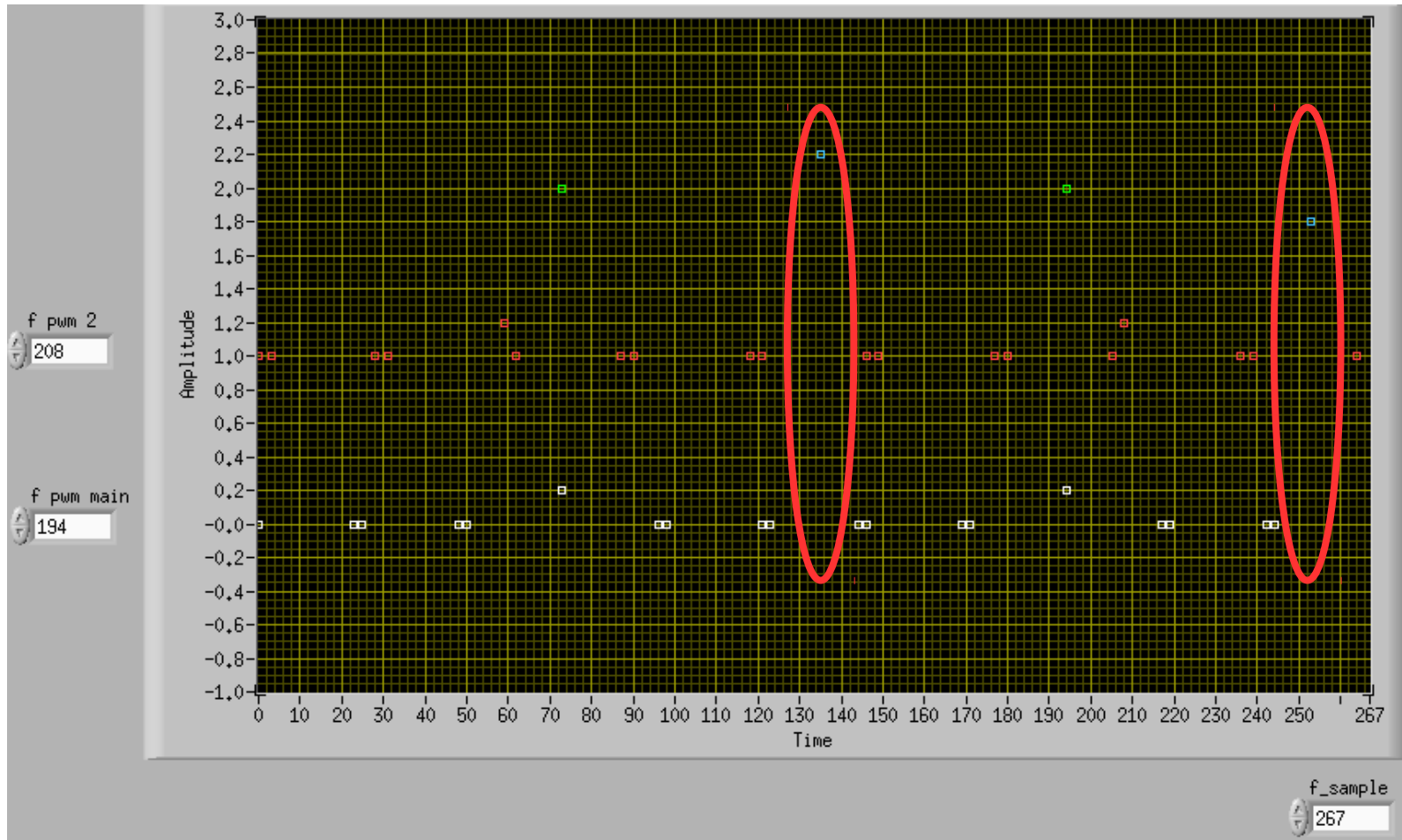
Here the main PWM frequency has around 1 kHz of 'empty space' around it.

Appendix E, frequency selection



No demodulation is done at the second PWM frequency, so it is allowed to obscure itself. The aliased harmonics close to the fundamentals (as shown in the red circles) are therefore no problem. The second PWM frequency must however not place any components close to the main PWM fundamentals.

Appendix E, frequency selection



For the 0/180 decision either the sum or difference frequency of the main and second PWM frequencies can be used. They are indicated by the blue dots, with the sum on the 2.2 line and the difference on the 1.8 line. The one used should not be obscured by any of the main or second PWM frequency components.

Appendix F, hardware used and demo videos

The hardware is that of a conventional sensorless FOC motor controller, with the addition of some basic opamp circuitry (the LNA):

- microcontroller: Microchip 33EV128GM006
 - running at 70 MIPS (max saliency based motor speed achieved: 12k-erpm)
 - 25 kB ROM code for a fully functioning controller, including transitions between saliency FOC and bempf based FOC, RS232 communication etc.
- current sensors: ACS770-100B
- LNA opamps: MCP6022, generic type with 10MHz GBW
- gate drivers: IRS 2186
- output stage: 6 FET, IXTH 180 (500 nsec deadtime)
- drill used for full torque experiments: Black&Decker BL186
- youtube video, drill, saliency only: [8Xz3RIYyQIQ](https://www.youtube.com/watch?v=8Xz3RIYyQIQ)
- youtube video, drill, saliency and BEMF: [8KOiBHHkPI4](https://www.youtube.com/watch?v=8KOiBHHkPI4)